Influence of variability of material mechanical properties on seismic performance of steel and steel-concrete composite structures

Badalassi, Massimo; Braconi, Aurelio; Cajot, Louis-Guy; Caprili, Silvia; DEGEE, Herve; Guendel, Max; Hjiaj, Mohammed; Hoffmeister, Benno; Karamanos, Spyros A.; Salvatore, Walter & Somja, Hugues (2017) Influence of variability of material mechanical properties on seismic performance of steel and steel-concrete composite structures. In: Bulletin of Earthquake Engineering, 15(4), p. 1559-1607.

DOI: 10.1007/s10518-016-0033-2
Handle: http://hdl.handle.net/1942/23660

Influence of variability of material mechanical properties on seismic performance of steel and steel-concrete composite structures

Massimo Badalassi[1], Aurelio Braconi[2], Louis-Guy Cajot[3], Silvia Caprili[1], Hervé Degee[4], Max Guendel[5], Mohammed Hjiaj[6], Benno Hoffmeister[7], Spyros A. Karamanos[8], Walter Salvatore[1], Hugues Somja[6]

[1]Thy Marcinelle - Rivagroup, Charleroi, Belgium
aurelio.braconi@gmail.com

[2] Department of Civil and Industrial Engineering University of Pisa, Italy
massimobadalassi@alice.it, silvia.caprili@ing.unipi.it, walter@ing.unipi.it

[3]Arcelor Mittal S.A.
lg.cajot@arcelormittal.com

[4] Faculty of Engineering Technology, University of Hasselt, Belgium
herve.degee@uhasselt.be

[5] Wölfel Beratende Ingenieure GmbH+ Co. KG, Höchberg, Germany
Guendel@woelfel.de

[6] Institut National des Sciences Appliquées de Rennes, France
Mohammed.Hjiaj@insa-rennes.fr, Hugues.Somja@insa-rennes.fr

[7] RWTH Aachen University, Institut für Stahlbau, Aachen, Germany
hoff@stb.rwth-aachen.de

[8] University of Thessaly, Volos, Greece
skara@mie.uth.gr

Abstract

Modern standards for constructions in seismic zones allow the construction of buildings able to dissipate the energy of the seismic input through an appropriate location of cyclic plastic deformations involving the largest possible number of structural elements, forming thus a global collapse mechanisms without failure and instability phenomena both at local and global level. The key instrument for this purpose is the capacity design approach, which requires an appropriate selection of the design forces and an accurate definition of structural details within the plastic hinges zones, prescribing at the same time the oversizing of non-dissipative elements that shall remain in the elastic field during the earthquake. However, the localization of plastic hinges and the development of the global collapse mechanism is strongly influenced by the mechanical properties of materials, which are characterized by an inherent randomness. This variability can alter the final structural behaviour not matching the expected performance. In the present paper, the influence of the variability of material mechanical properties on the structural behaviour of steel and steel/concrete composite buildings is analyzed, evaluating the efficiency of the capacity design approach as proposed by Eurocode 8 and the possibility of introducing an upper limitation to the nominal yielding strength adopted in the design.

Keywords

Probability of failure, capacity design, steel and steel/concrete buildings, overstrength factor, variability of material mechanical properties

1. Introduction

Actual seismic design standards for steel and steel/concrete composite buildings are based on the capacity design approach (EN1998-1:2005, FEMA356:2000, D.M.14/01/2008), aiming at developing global ductile collapse mechanisms, for the different structural typologies, through the localization of cyclic plastic deformations in correspondence of specific energy dissipative regions (*plastic hinges*). The capacity design approach prescribes the sizing of specific “dissipative structural elements” (i.e. beams in Moment Resisting Frame structures – MRF, links in Eccentrically Braced Frames – EBF, braces in Concentrically Braced – CBF) using conventional solicitations and oversizing the remainders, such as columns and braces, that shall keep an elastic behaviour, i.e. not dissipating any energy.

In the Eurocode 8 design procedure (EN1998-1:2005) the oversizing of these non-dissipative elements is obtained increasing their design solicitations through two overstrength coefficients: the *material* overstrength factor (γ_{ov}), representing the ratio between the real and the nominal values of yielding strength, and the *design* overstrength factor (Ω), that is the minimum ratio between the plastic design strength of the dissipative element and the corresponding solicitation coming from seismic load combination. In particular, the γ_{ov} coefficient is assumed equal to 1.25 for all the steel grades as default case when no experimental measured values are available; however, this is in contrast to what actually reported in the Italian seismic code (D.M.14/01/2008) in which the material overstrength coefficient varies as a function of the steel grades.

The material overstrength factor (γ_{ov}) together with the design one (Ω) contribute to size the protected elements; for example, the columns of MRF are designed using conventional solicitations defined as $E_{column,i} = E_i^{gravity} + 1.1 \cdot \gamma_{OV} \cdot \min \Omega_j \cdot E_i^{seismic}$, in which the contribution of seismic action ($E_i^{seismic}$) is amplified adopting both the overstrength factors (EN1998-1:2005; D.M.14/01/2008). Variability of the mechanical properties of materials (i.e. yielding strength) so plays a key role in determining the real collapse modes: if not properly controlled, it may alter the localization of plastic hinges compared to the results of the capacity design, leading to a lower seismic energy dissipation and to an unexpected global behaviour of the building.

The γ_{ov} is introduced to reduce the influence of the material variability on the capacity design approach, while Ω factor, that is mainly a 'structural' factor taking into consideration the difference among demand and capacity of structural elements.

However, inconsistencies between the design standards for steel and steel-concrete composite buildings and the production standard still exist. For instance, EN10025:2004 does not prescribe the adoption of an upper limitation to yielding strength for the concerned steel grades: this translates into effective value of yielding strength also higher than $\gamma_{ov} \cdot f_{y,nom}$, varying thus the collapse mechanisms designed through the capacity design approach (EN1998-1:2005).

Several studies in the current scientific literature deal with the influence of material variability in the structural behaviour of buildings designed in seismic areas. Elnashai and Chryssanthopoulos (1991) examined the effect of random material variability on the structural response of buildings under earthquake loading conditions, applying a statistical procedure to a simple MRF portal frame, aiming to evaluate the consequences of such scatter on the weak beam/strong column scheme adopted following the capacity design approach and possible implications for design codes. Rossi and Lombardo (2007) analyzed the influence of the design overstrength of the seismic link on the behaviour of EBF designed in accordance with capacity design principles; deterministic design values of yield strength were mainly assumed, while some random analyses were also carried out to achieve an accurate check of capacity design and a global understanding of the sensitivity of the structural response to real strength distributions. Obtained results highlighted the frequent concentration of plastic deformation in few storeys due to the high scatter of normalized γ_{ov} and a performing behaviour of EBF if the scatter is anyway limited to 1.25, according to EN1998-1:2005.

Badalassi et al. (2013) deeply investigated the effects of variability of the material properties and of the seismic input on the ductile behaviour of EBF steel structures, allowing to evaluate the efficiency of the capacity design approach in predicting the real seismic performance of such constructions and the influence of material scattering in the activation of collapse modes.

Within this technical context, a European research project funded by the Research Fund for Coal and Steel (RFCS), "OPUS – *Optimizing the seismic Performance of steel and steel-composite concrete structures by Standardizing material quality control*" (Braconi et al. 2013), was carried out. The project aimed at investigating the influence of material properties variability on the ductile behaviour of different steel and composite steel/concrete structural types (MRF, CBF and EBF) designed according to the Eurocodes (EN1990:2005; EN1991-1-1: 2005; EN1992-1-1:2005; EN1993-1-1:2005; EN1994-1-1:2005; EN1998-1:2005). The behaviour of the designed structures was analyzed through Incremental Dynamic Analyses (IDA) adopting material properties generated using a probabilistic model realized using actual production data (Badalassi et al. 2011, Badalassi et al. 2013, Braconi et al. 2015, Somja et al. 2013).

The results were presented in terms of activation probability for each relevant collapse criteria, analyzing the variation of the structural safety level as function of the demand imposed by the earthquake and of the material properties. The generated results also allowed: to assess the structural performance of buildings in terms of behaviour factor *q* (Braconi et al. 2013, Braconi et al. 2015); to measure the impact of imposing upper limitations to the yielding stress of steel grades through additional quality control; to evaluate the efficacy of the capacity design approach for the protection of dissipative members through the adoption of the overstrength coefficients, γ_{ov} and Ω.

In the present paper the main results of aforementioned OPUS project (Braconi et al. 2013) are illustrated with particular reference to the influence of materials properties variation on the seismic performance of steel and steel-concrete structures. The analysis was performed combining different lateral resisting systems (MRF, EBF and CBF), different steel qualities (S235, S275, S355 and S460) and adopting bare steel and steel-concrete composite solutions. 15 tri-dimensional structures were designed and their mechanical response and collapse modes accurately characterized.

A suitable probabilistic procedure was then set-up in order to estimate the failure probability associated to the identified collapse modes and a probabilistic model of the mechanical properties – f_y, f_t, ε_u – of the European structural steel products (profiles, plates and reinforcing bars) was accurately developed and calibrated.

2. The proposed probabilistic procedure

Reliability problems in earthquake engineering are often characterised by non-linear limit-state functions, with high curvatures and multiple design points. Robust procedures shall be then applied to achieve reliable results: some of them are briefly presented in the following, aiming to define a correct methodology to be used in the present work.

The structural failure during an earthquake occurs when the capacity (C) is exceeded in one or more elements by the demand (D), being both C and D time-dependant and mutually inter-dependant: the failure of the whole structure is related to the sequence of collapses occurring in the structural elements. In this context, a complete non-linear time-dependant seismic reliability analysis should use random processes leading, in many cases, to excessive and time demand computing (Somja et al. 2013).

In the common practice, the time-variant approaches are not applicable to the seismic reliability due to the complexity of the problem, which becomes extremely high for nonlinear systems.

The practical applications of the seismic reliability follow time-integrated approaches, in which the maximum response of all critical elements is collected neglecting their not simultaneous responses: from a practical point of view, this means that, for each seismic input, the maximum response of selected parameters (i.e. base shear, displacement and so on) has been considered, even if not achieved in correspondence of the same instant of the accelerogram.

Time is implicitly integrated in the collected variables and the definition of collapse criteria is identified by predefined values, taking into account the mechanical properties of the materials and the features of the structural typology.

In this framework, FORM and SORM methods (Denoel 2007, Spaethe 1992, Breitung 1984), that are considered as valuable for codes calibration and reliability problems on simple systems, have a limited efficiency. Simulations methods, on the other hand, appear to be more reliable, because not usually requiring “a-priori” knowledge of the limit state function. However, they need a large number of numerical analyses to estimate, with a sufficient accuracy, the probability of failure.

In last decades, many optimization techniques devoted to the improvement of simulation methods have been defined in order to reduce the computational work. Importance sampling is one of most used and appears to be a promising one in failure probability estimation although it requires the knowledge of the failure domain in order to generate samples for carrying out the probabilistic analyses with the necessary accuracy. Many other methods based on the same approach have been proposed as for instance Directional Simulations and Adaptive Sampling. Moreover, other methods essentially based on a statistical interpretation of the results have been also developed. Those techniques, as for instance the Surface Response focus the attention on the definition of an appropriate function linking structural response (output variables) to seismic hazard/material variability (input variables). However, these techniques are characterized by one of the previous weaknesses, i.e. predicting the response around the design point.

Therefore, direct simulation methods as Monte Carlo, although time demanding and requiring a thorough knowledge of the structural system under examination, are a reliable technique for estimating the failure probability. It is also evident that the knowledge of the structural system – number of design points; limit-state functions; probabilistic variables; dependence and interdependence among variables – represents the basis for a successful or unsuccessful application of Monte Carlo method.

Basing on these considerations, for the purposes of the present study, a time-integrated approach was adopted within the following seismic reliability framework:

- *Step 1*. ***Knowledge***. The deep knowledge of structural systems was obtained through numerical simulations - non-linear static and dynamic analyses – and the identification of collapse modes.
- *Step 2*. ***Collapse criteria***. For each structural typology, the relevant collapse criteria at global and local level were defined through an accurate analysis of the outcomes of the Step 1.
- *Step 3*. ***Probabilistic variables***. A probabilistic model for the generation of samples of the mechanical properties was defined. The scattering of steel mechanical properties was represented by a multi-variable model in which the yielding strength $R_{e,H}$ (f_y), the tensile strength R_m (f_t) and the elongation at fracture A (ε_u) were considered with their probabilistic interdependencies.
- *Step 4*. ***Seismic hazard and input***. Seismic actions were modelled adopting the hazard model proposed by EN1998-1:2005 calibrated according to design parameters associated to ultimate limit states (ULS). According to this choice, the response spectrum proposed by Eurocode 8 (EN 1998-1:2005) was assumed to generate seven seismic inputs to be adopted during the non-linear time-history analyses. In such context, the peak ground acceleration (PGA) was chosen as intensity measure (IM).
- *Step 5*. ***Numerical simulations***. The correlation between the seismic demand and the structural response of case studies was defined through non-linear dynamic analyses. The PGA was increased up to the level corresponding, for each different seismic input, to the activation of relevant collapse modes, identified in Step 1 and Step 2.
- *Step 6*. ***Probabilistic procedure***. The results of the dynamic analyses were analyzed employing a statistical procedure aimed at constructing the fragility curves and yearly threshold exceedance probability of the relevant collapse modes for each case study. The probability of failure for each case study, P_{fail}, was finally estimated.

3. Design and modelling of case-studies

3.1 Seismic design of case study buildings

A representative set of case study buildings (i.e. MRF, CBF and EBF using steel and steel-concrete composite solutions), housing different activities, was designed according to Eurocodes; some examples of the general schemes of designed buildings are presented in the Figure 1. Two levels of design seismic actions were adopted: low and high seismic hazard, with peak ground acceleration (PGA) equal to 0.10-0.15g (low) and 0.25g (moderate). Static loads were evaluated according to Eurocode 1 (EN1991-1-1:2005) adopting the same wind action for all structures. Table 1 summarizes the information related to the use category, live and environmental loads (snow, wind and earthquake) and floor typologies, whereas geometry and resisting systems are listed in Table 2.
The design procedure was carried out in agreement with European and international standards (EN1998-1:2005, EN1991-1-1:2005, EN1990:2005, EN1993-1-1:2005, EN1994-1-1:2005, EN1998-3:2005, EN1992-1-1:2005). A procedure aiming at optimizing elements' dimensions and at avoiding over-sized structural members was subsequently applied, especially for limiting the over-sizing on seismic design induced by wind loads higher than seismic ones. The "optimal design" was not always reached due to design rules and limitations imposed by Eurocodes.

Table 1: Structural typologies and design loads used for case studies.

ID	Type	Material	Live (kN/m^2)	Snow (kN/m^2)	Wind (kN/m^2)	PGA (g)	Slab typology	Mass
1	Office	Steel	3,00	0,85	0,39	0,10	composite 18 cm (not des.)	2975 t
2	Office	Steel	3,00	0,85	0,39	0,10	composite 18 cm (not des.)	2975 t
3	Office	Steel	3,00	1,00	1,10	0,25	concrete slab cast on prefabricated trussed slab, 23 cm, wire mesh 1 ϕ8/150 mm, bars 2ϕ10 / slab rib.	1747 t
4	Office	Steel	3,00	1,00	1,10	0,15	concrete slab cast on prefabricated trussed slab, 23 cm, wire mesh 1 ϕ8/150 mm, bars 2ϕ10 / slab rib.	1747 t
5	Office	Steel	3,00	1,40	(30 m/s)	0,25	concrete, 12 cm (not des.)	1000 t
6	Office	Composite beams/ Steel columns	3,00	1,11	1,40	0,10	concrete, 12 cm - reinf. 3/m - 5ϕ10 (X) and 5ϕ8 (Y), upper and lower layer.	1916 t
7	Office	Composite beams and columns	3,00	1,11	1,40	0,10		1995 t
8	Office	Composite beams/ Steel columns	3,00	1,11	1,40	0,25		1909 t
10	Office	Composite beams/ Steel columns	3,00	1,11	1,40	0,10	concrete 18 cm - upper reinf. (X) 10ϕ10+4ϕ16, (Y) 10ϕ10; lower reinf. 10ϕ10 +2ϕ16 (X), 10ϕ10 (Y).	1750 t
11	Office	Composite beams and columns	3,00	1,11	1,40	0,25	Conc.18 cm - upper reinf. (X) 10ϕ10+4ϕ16, (Y) 10ϕ10; lower reinf. 10ϕ10 +4ϕ16 (X), 10ϕ10 (Y).	1745 t
12	Industrial	Steel	5,00	1,40	(30 m/s)	0,25	concrete 24 cm (not des.)	0,3Q+150 t
13	Industrial	Steel	Crane load (10 tons)	1,40	(30 m/s)	0,25	-	350 t
14	Industrial	Steel	Crane load (510 tons)	0,85	0,39	0,25	-	792 t
15	Industrial	Steel	5,00 kN/m^2 + dead loads (6,8 kN/m^2)	0,85	0,39	0,10	composite 18 cm (not des.)	4107 t
16	Car Park	Steel	2,50	1,00	1,10	0,25	concrete slab cast on prefabricated trussed slab, 23 cm, wire mesh 1 ϕ8/150 mm, bars 2ϕ10 / slab rib.	5761 t

Table 2: Structural and geometrical characteristics of designed case studies.

ID	Storeys	X – direction				Y – direction			
		System	Span	Second. beam	H_{storey} [m]	system	Span	Second. beam	H_{storey} [m]
1	5	MRF	3x7m	Yes	3,5	CBF	4x6m	No	3,5
2	5	CBF	3x7m	Yes	3,5	CBF	6x6m	No	3,5
3	5	EBF shear	3x7m	No	3,5	EBF shear	4x6m	Yes	3,5
4	5	EBF bending	3x7m	No	3,5	EBF bending	4x6m	Yes	3,5
5	5	MRF	3x7,5m	Yes	3,5	CBF	4x6m	Yes	3,5
6	5	MRF	3x7m	Yes	3,5	Not designed	4x6m	No	3,5
7	5	MRF	3x7m	Yes	3,5	Not designed	4x6m	No	3,5
8	5	MRF	3x7m	Yes	3,5	Not designed	4x6m	No	3,5
10	5	EBF shear	3x7m	No	3,5	CBF	4x6m	No	3,5
11	5	EBF shear	3x7m	No	3,5	CBF	4x6m	No	3,5
12	4	MRF	3x7,5m	Yes	4+4+5+7	CBF	3x10m	No	4+4+5+7
13	1	MRF	2x25m	Yes (purlins)	10,5	CBF	11x6m	Yes (purlins)	10,5
14	1	MRF truss girder	1x29m	No	21,9	CBF	7,30m	No	17,6
15	4	MRF	3x7,5m	No	4+4+5+7	CBF	3x10m	Yes	4 +4 + 5+7
16	2	EBF shear	5x8m 2x10m	No	4+4	EBF shear	6x10.5m	Yes	4+4

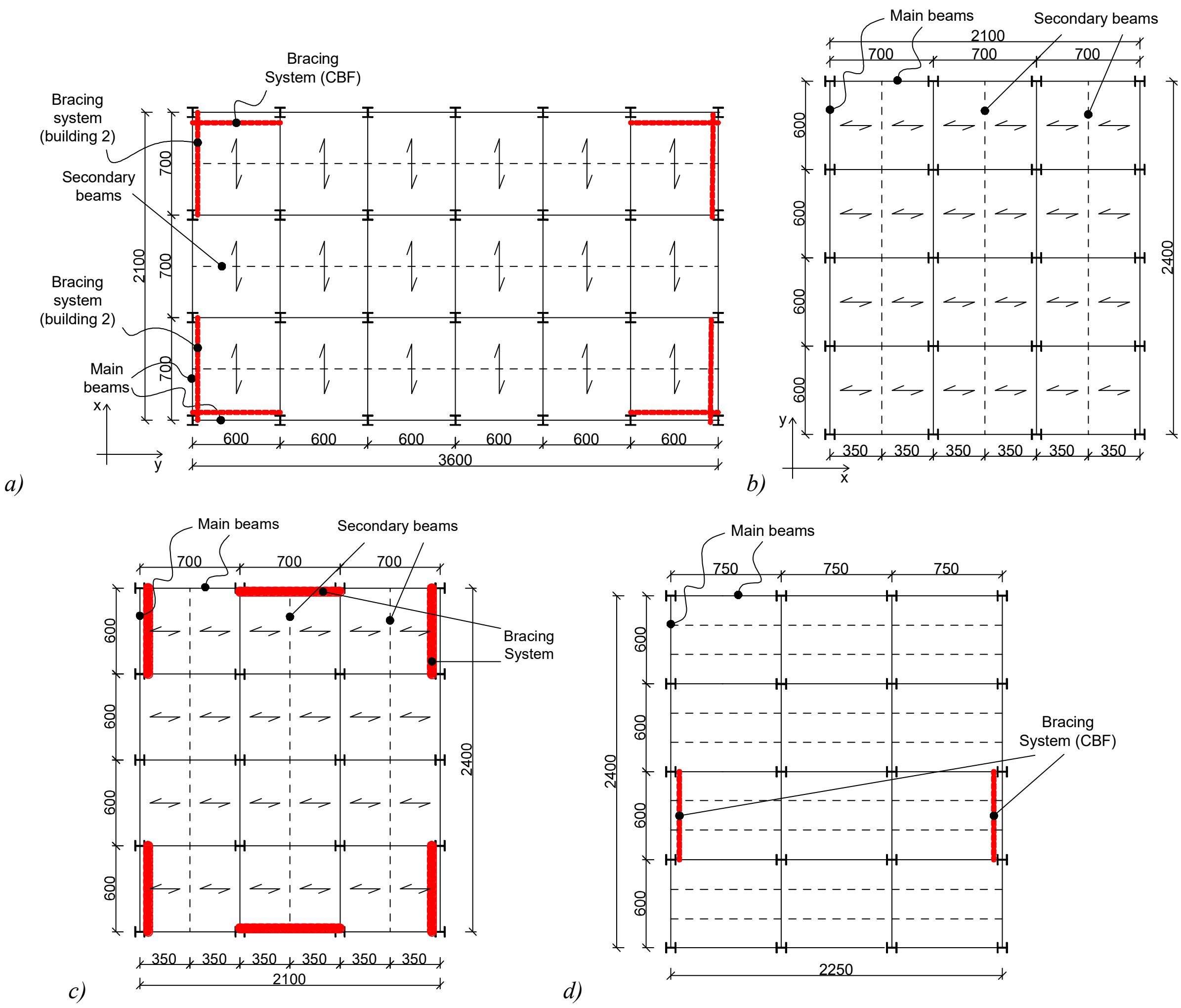

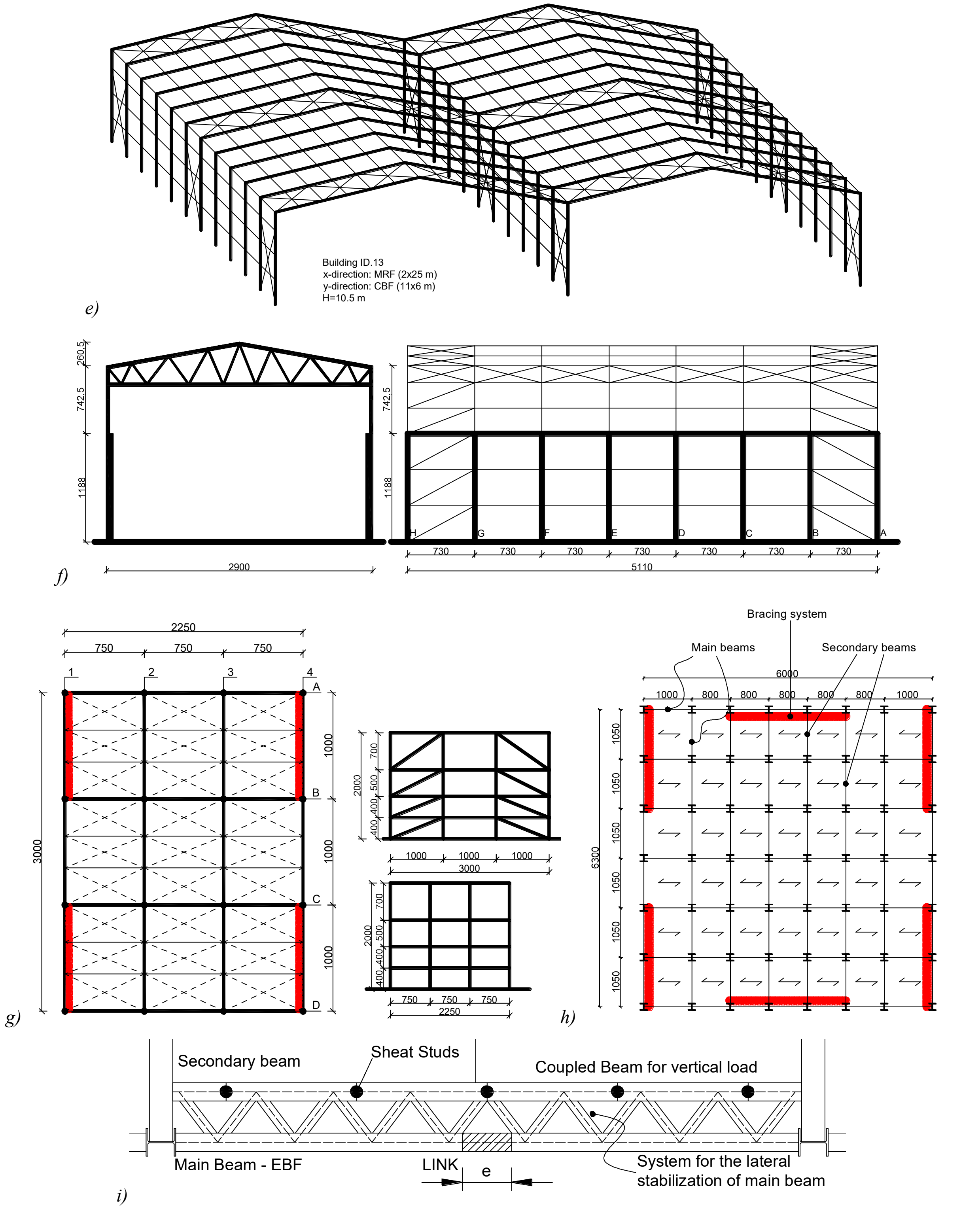

Figure 1: a) buildings 1-2, d) buildings 6, 7, 8, 10, 11 (MRF and MRF-CBF), c) buildings 3, 4 (EBF or CBF), d) building 5, e) building 13, f) building 14 (MRF and CBF), g) buildings 12 and 15 (MRF and CBF), h) building 16 (EBF), i) beam duplication for decoupling vertical and seismic loads.

MRF structures were designed considering columns fixed at the base and adopting full strength rigid joints, while pinned connections were used for the design of braced frames (both EBF and CBF). The design of MRFs for static load combinations leaded to over-sized beams respect to the simple seismic strength's requirements and the same effect was detected for EBFs as well. Moreover, the final design of protected elements, such as the columns of MRFs, was strongly influenced by the seismic design composed by capacity design approach, drift limitations and the sensitivity to second order effects (θ):

$$E_i^{c.d.} = E_i^{gravity} + 1.1 \cdot \gamma_{OV} \cdot \min(\Omega_j) \cdot E_i^{seismic} \quad (1)$$

$$\sum M_{Rd,PL}^{column} \geq 1.3 \cdot \sum M_{Rd,PL}^{beam} \quad (2)$$

$$\nu \cdot q_d \cdot d_e = \nu \cdot d_r \leq d_{LIMIT} \quad (3)$$

$$\theta = \frac{P_{tot} \cdot d_r}{V_{tot} \cdot h} \leq \beta \quad (4)$$

being: $E_i^{gravity}$ the effect on the i-th member due gravitational loads; $E_i^{seismic}$ the effect on the i-th member due to the seismic action; $E_i^{c.d}$ the effects on the i-th member coming from the capacity design approach; γ_{ov} the material over-strength (default value at 1.25); $M_{Rd,PL}^{column}$ and $M_{Rd,PL}^{beam}$ the design resistant bending moments of columns and beams; d_r the drift coming from the analysis using the design response spectrum; d_e the elastic drift coming from analyses and d_{LIMIT} its maximum allowed value;ν the reduction factor associated with the damage limitation (DL) condition; q_d the displacement behaviour factor; P_{tot} and V_{tot} respectively the total vertical actions and the horizontal ones on the i-th floor; θ the sensitivity factor to second order effects.

The Ω factor represents the structural over-strength of the non-dissipative members designed to remain in the elastic field during earthquake, compared to dissipative ones, which undergo plastic deformations. The Ω factor is defined according to the following equation:

$$\Omega_i = \alpha \cdot \frac{R_{d,i}}{E_{i,dissipative}^{seismic}} \quad (5)$$

being α a coefficient equal to 1.0 for MRFs and CBFs and 1.5 for EBFs, while $R_{d,i}$ is its plastic resistance and $E_{i,dissipative}^{seismic}$ is the maximum level of solicitation induced by the seismic combinations.

The over-sizing of non-dissipative members and the adoption of limitations for interstorey drift ratio increased thus the size of columns and beams, respect to what effectively required by the seismic loading condition. To solve this problem, an appropriate design process seeking behaviour factor harmonized with strength requirements coming from static load combinations was followed. The procedure leaded to the adoption of lower q factors with respect to what suggested by standards.

In the case of EBFs the control of the links' over-sizing was checked considering that difference amongst Ω_i of all links shall not exceed the 25%, according to equation (6):

$$\frac{\Omega_{max}}{\Omega_{min}} \leq 1.25 \quad (6)$$

where Ω_{max} and Ω_{min} are respectively the maximum and the minimum values of the structural over-strength factors for the dissipative members. In order to decouple static effects from seismic effects on links and to reduce the design over-strength, beams containing links were coupled with parallel beams to which the entire vertical loads were assigned. This solution allowed the optimization of the seismic links (beams), reaching a utilization ratio equal to 1.0 and over-strength coefficient Ω up to 1.5 in seismic load combinations. This optimisation resulted, however, in bigger bracing sections and the EBF final design was also heavily influenced by second order effects by buckling control in compressed members.

Concerning CBF solutions, the design process proposed by EN1998-1:2005 obliged to perform an accurate design in order to satisfy limitation related to brace slenderness ratio (λ):

$$1.3 \leq \lambda \leq 2.0 \quad (7)$$

and the assessment of equations (1), (3) and (4). In some cases, it was possible to optimise the design; for all the others, it was necessary to adopt, for bracings, different steel qualities at different floor levels.

The design of steel-concrete composite structures was executed in agreement with Eurocodes' prescriptions (EN1998-1:2005, EN1990:2005, EN1994-1-1:2005) and with the evidences and results in the scientific literature (Braconi et al. 2008, Braconi et al. 2008b). Lateral torsional buckling was supposed to be prevented for beams as well as for columns, in order to ensure a stable behaviour of the members during the development of the plastic hinges. All columns were designed with the increased solicitations coming from the capacity design in order to respect the strong column-weak beam principle for MRFs.

The previous design procedures such as the adoption of different steel grades for braced configurations, the selection of optimized behaviour factors for MRFs and the remainders are not commonly adopted in the current engineering design practice. Thus the default procedure of Eurocode 8 (EN1998-1:2005) can lead to over-sized structural solutions which have higher performance than those required by the seismic demand. In particular, the capacity design approach works in this sense giving structural solutions not fully optimized (Braconi et al. 2015). More details regarding the design of case studies can be found in Badalassi et al. (2013) and in Opus Final report (Braconi et al. 2013b).

3.2 Numerical modelling of the case study buildings

Numerical analyses of buildings 1, 2, 14 and 15 were carried out by using Dynacs software (Kuck and Hoffmeister, 1993). The structures were modelled using bi-dimensional frames with fibre beam elements and adopting a bi-linear stress-strain law with kinematic hardening. The braces were modelled through non-linear spring elements, able to represent the elastic-plastic cyclic behaviour under tension, the global buckling under compression and the cyclic degradation. Large deformations and P-Δ effect were considered.

Composite steel/concrete structures (buildings 6, 7, 8, 10 and 11) were modelled with FineLG software (2003), using fibre beam elements for the steel part and other fibre elements for the concrete one. The diagonal members of EBF and CBF structures were modelled using steel beam element including lateral buckling phenomena under compression. The seismic links were modelled through a classical non-linear beam element, with shear deformation included; the parameters of the beam were calibrated using a refined FEM model. Buildings 5, 12 and 13 were modelled using Abaqus software (2005), adopting 3-node quadratic beams in plane for beams and columns and 3-node quadratic beams in space for concentrically braced frames. An elastic-plastic model with linear kinematic hardening was used to model the steel structural elements.

Buildings 3, 4 and 16 were modelled using OpenSees software (Mazzoni et al. 2007) and fibre elements for all the structural members. The buckling phenomena of compressed members were introduced providing an initial imperfection (1/500 of the brace length) to the middle point of the brace and an initial imperfection to the top of the columns. The Menegotto-Pinto (1973) law was used to model flexural behaviour of elements, while for the shear deformation of the links, a bilinear elasto-plastic with hardening force-angular distortion law was adopted.

The reliability of adopting different software for the modelling and the numerical analyses of case study buildings was deeply assessed in the main framework of the Opus project (Braconi et al. 2013b), since strictly connected to the analysis of results and the following conclusions. To this purpose, three benchmark structures (i.e. a brace element with different sections, a portal frame and a portal frame with bracing system) were modelled and subjected to monotonic and cyclic pushover analyses, as described in Braconi et al. (2015), showing a good agreement of the results obtained from the adoption of the four software Dynacs, FineLG, Abaqus and OpenSees. It is moreover to be noted that the considered case studies (i.e. MRF, CBF and EBF steel and steel-concrete composite structures) represent typical and standard structures designed following the principles of the capacity design approach and consequently characterized by a linear behaviour everywhere except for the dissipative zones: that nonlinear behaviour (and eventual difficulties related to modelling) is then strictly limited to specific zones, deeply calibrated (think for example to the example of the calibration of the brace element for CBF case studies). As a consequence, and in relation to what deeply described in Braconi et al. (2015) the calibration procedure of software was considered sufficient for assuring the reliability of results.

Figure 2 presents some examples of three-dimensional models elaborated for the case studies; more details regarding the elaboration of the numerical models can be found in Opus final report (Braconi et al. 2013b), Braconi et al. (2015) and Badalassi et al. (2013).

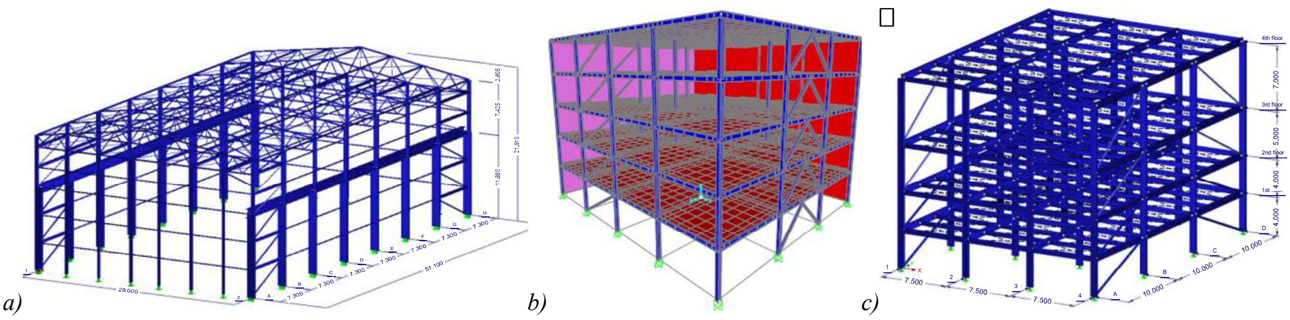

a) *b)* *c)*

Figure 2: a) Industrial building; b) EBF and CBF configurations for offices; c) MRF and CBF configurations for industrial storage

3.3 Structural performance of designed buildings: selection of collapse criteria

Seismic demand was defined in relation to performance levels such as Damage Limitation (DL), Severe Damage (SD) and Near Collapse (NC). The definition of the limit states and of the associated structural performance under seismic actions was necessary to correctly understand the structural behaviour. As general rule, deformation criteria (i.e. the over-passing of the interstorey drift limit, the reaching of the ultimate rotation of beams…) or local ductility criteria were selected as main indicators.

Non seismic-specific assessments (i.e. shear capacity of brittle elements, global buckling) were also considered. The global deformation criteria as roof and storey drift were defined according to FEMA356 (2000) and used only as indicative values: this means that these limitations are not mandatory according but were anyway taken into consideration in the present work. Additionally, the maximum forces acting in the connections and at foundation level were obtained for further investigations but not directly used in the present work. Limit states considered for MRF, CBF and EBF are presented respectively in Table 3. More details and information can be found in Braconi et al. (2013b), Braconi et al. (2015) and Badalassi et al. (2013).

Table 3: Failure criteria for buildings (*) for axial load ration 0.3 < n ≤ 0.5 linear reduction of rotation capacity in acc. to FEMA356; (**) Lateral torsional buckling of beams is prevented by RC-floor.

	Type	Reference	Criteria	Structural typology	Values considered
A	Dynamic instability (Global)	-	Mandatory	MRF, CBF, EBF	-
B	Maximum roof drift ratio (Global)	FEMA 356	Indicative	MRF, CBF, EBF	Collapse Prevention: 5 % transient or permanent Life Safety: 2.5 % transient; 1 % permanent Immediate Occupancy: 0.7 % transient; negligible permanent
C	Inter-storey drift ratio (Global)	FEMA 356	Indicative	MRF, CBF, EBF	Not specified values according to FEMA 356. Refer to roof drift ratio (explanation below).
D	Ultimate rotation of plastic hinges (Local) *	EN1998-3	Mandatory	MRF*, CBF	Refer to Eurocode 8
E	Shear capacity (Local)	EN1993-1	Mandatory	MRF, CBF, EBF	Refer to Eurocode 8
F	Lateral torsional buckling (Local) **	EN1993-1	Mandatory	MRF, CBF	Refer to Eurocode 8
G	Global buckling (Local)	EN1993-1	Mandatory	MRF, CBF, EBF	Refer to Eurocode 8
H	Joint forces	-	To evaluate	MRF, CBF, EBF	-
I	Foundation forces	-	To evaluate	MRF, CBF, EBF	-
N	Ultimate rotation of link (Local)	FEMA 356	Mandatory	EBF	For shear links: 110 mrad For bending links: 20 mrad

To better specify what is presented in Table 3 concerning the limitations for the interstorey drift ratio, it is necessary to underline that FEMA 356 does not provide any limit values for such parameter. Nevertheless, in the case studies analyzed in the present paper, the limits for roof displacement are used as interstorey drift criterion. The interstorey drift does not show directly the collapse of the building, but the limits are based on the experience of former earthquakes. Hence, the interstorey drift is considered as 'indicative value' and shall be checked against proposed limits in EN1998-1:2005 and FEMA 350.
Moreover, according to the approach adopted in the present work, the expression "indicative" means that the considered criterion is not mandatory but was anyway followed and considered for nonlinear analyses, since representative for the considered structure. The expression "To evaluate" means that the considered criterion, even if important and relevant for the considered structure, was not introduced in the analyses since no sufficient information are present (for example, joint forces for the design of connections, forces adopted for the design of foundations and so on).

4. Modelling of material property variability

The analysis of the variability of material properties for different steel products was carried out on the basis of production data kindly furnished by some industrial producers. Statistical investigations were carried out organizing collected data in homogeneous classes, according to what proposed by production (EN10025:2004, UNE 36065: 2000, AFNOR NFA 35-019-1-11/2007,D.M. 14/01/2008) and design standards (EN1998-1:2005, EN1993-1-1:2005, EN1992-1-1:2005).
Data collected by industrial producers were related to steel reinforcing bars, structural steel profiles and steel plates. The set of all investigated steel products is reported in Table 4, Table 5 and Table 6; steel grades, reference production standards and information on geometrical parameters are also listed. For sake of completeness, the statistical parameters were compared with information and modelling parameters used in a previous research (*PROQUAM*, Cajot et al. 2005) or suggested as suitable for probabilistic evaluation of structural safety (*JCCS*, 2001).
The statistical analysis of collected data was performed adopting traditional procedures and was necessary for the elaboration of the probabilistic material model used for the generation of samples to adopt in numerical analyses. The model was defined as *multi-variables,* in which the statistical interdependencies between yielding stress, tensile strength and elongation at fracture were properly taken into account. The collection of data concerned the stress-strain curves obtained by industrial partners during quality checks as well: a database was created and elaborated in order to define simple correlations between the key points of the stress strain curves and the probabilistic variables (f_y, f_t, A_{gt} or ε_u). The

stress-strain curve coming from the industrial quality checks was calibrated and compared with some experimental results coming from *PLASTOTOUGH* research project (Schäfer et al. 2010).

Table 4: Collected data for steel reinforcing bars.

Diameters [mm]	Steel grade	Production Standard
8, 10, 12, 14, 16, 18, 20, 22, 24, 26, 28, 30, 32	B450C	Technical Code for Construction (2008) - Italy
8, 10, 12, 16, 20, 25, 32	S500SD	UNE 36065 (2000) - Spain
14, 16, 18, 20, 22, 25	B500B	AFNOR NF A35-019-1 (2007) - France

Table 5: Collected data for structural steel plates.

Thickness ranges [mm]	Steel grade	Production Standard
7÷16; 16÷40; 40÷63; 63÷80; 80÷100	S235J0/AR	EN 10025-2
7÷16; 16÷40; 40÷63; 63÷80; 80÷100	S275J0/AR	EN 10025-2
7÷16; 16÷40; 40÷63; 63÷80; 80÷100	S355J0/AR	EN 10025-2
7÷16; 16÷40; 40÷63; 63÷80; 80÷100	S355J0/W	EN 10025-5
16÷40; 40÷63	S460M	EN 10025-4

Table 6: Collected data for structural steel profiles.

Profile Series		Steel grade	Production Standard
HE 100 – 600	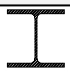	S235JR/J0	EN 10025-2
IPE 100 – 750	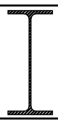	S275JR/J0 S275M	EN 10025-2 EN 10025-4
UPN 80 – 400	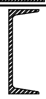	S355J0/J2/K2 S355M	EN 10025-2 EN 10025-4

4.1 Statistical analysis of industrial production data

A statistical analysis was executed on collected data in order to define mean (μ), standard deviation (σ), coefficient of variation (CoV), variances (σ^2_{xy}), upper and lower percentile ($X_{5\%}$ and $X_{95\%}$), Curtosi and Skewness indexes for each set of homogeneous steel products defined on the basis of indications contained in the production standard (in which steel grades and geometries are defined). In particular, among all the furnished data, the following mechanical properties of structural steels (profiles and plates) were analyzed:

- yielding stress ($R_{e,H}$ or f_y – EN1993-1-1:2005 and EN1998-1:2005).
- Ultimate tensile strength (R_m – EN10025:2005 or f_t –EN1993-1-1:2005 and EN1998-1:2005).
- Ultimate elongation (A – EN10025:2005 or ε_u - EN1993-1-1:2005 and EN1998-1:2005).

For steel reinforcing bars, the following mechanical properties were investigated:

- yielding stress (f_y – UNE 36065: 2000, AFNOR, NFA 35-019-1-11/2007, D.M. 14/01/2008).
- Ultimate tensile strength (f_t – UNE 36065: 2000, AFNOR, NFA 35-019-1-11/2007, D.M. 14/01/2008).
- Elongation at maximum load (A_{gt} – UNE 36065: 2000, AFNOR, NFA35-019-1-11/2007, D.M. 14/01/2008).

First order moments (μ) and second order quantity (σ) allowed a general comparison between the samples data set and the relative values proposed by production standards. The coefficient of variation (CoV) allowed the comparison between scatterings showed by different mechanical properties. The Curtosis and the Skewness indicators gave a picture of the shape of statistical distribution of observed samples, while variance and co-variance coefficients defined the correlation matrixes and the probabilistic interdependencies between observed mechanical parameters.

4.1.1 Structural steels for profiles, plates and steel reinforcing bars

The characterization of mechanical properties variability for the structural steel profiles concerned the following steels grades: S235AR(+M), S275AR(+M), S275M, S355AR(+M), S355M and S460M. Data related to structural profiles rolled according to series HEA, HEB, IPE, angles and channels were collected by different industrial producers (i.e. *Producer A, Producer B* and *Producer C*). Besides the steel profiles, data about structural plated elements were collected from *Producer B* as well.

The distribution of data of plates and profiles was not continuous and homogeneous across all steel grades and thickness classes according to the production standard EN10025:2004, due to the different requests made by the market to the

contributors in terms of qualities, thickness or product types. Sets characterized by low statistical meaning were then neglected. The statistical evaluation of the meaningful data was executed identifying first macro groups in terms of grade and thickness class as defined by EN10025:2004.The results of the statistical analysis are reported in the Appendix, from Table A 1 to Table A 6 and in the corresponding Figures (from Figure A 1 to Figure A3).
Data related to reinforcing bars (Table 8A), obtained from three different plants in Italy (for steel grade B450C), Spain (for steel grade B500SD) and France (for steel grade B500B), were grouped using the nominal diameter as parameter. The mechanical properties assumed as variables for the characterization of each macro-group were selected according to Eurocode 2 (EN1992-1-1:2005): yielding stress – f_y ($R_{e,H}$), tensile strength – f_t (R_m) and elongation at maximum load – A_{gt} (ε_{uk}).

4.1.2 Concrete properties

A European producer kindly furnished its collected data on concrete properties. The concrete strength classes analysed in the project were only those used in the design of the steel-concrete composite case-studies. The unique mechanical property of the concrete assumed as probabilistic variable was the maximum compressive strength. The statistical data of the concrete strength classes are represented in the Appendix (Table A 7).

4.2 Probabilistic model and generation of samples

The adopted probabilistic model was based on a multi-varied Gaussian system, correlating Gaussian variables of such system with Log-Normal functions describing the probabilistic laws of all the observed material properties (f_y, f_t and A_{gt}) as follows. Given two vectors of scalar random variables, X and Y:

$$X = [x_1 ... x_n] \quad (8)$$

$$Y = [y_1 ... y_n] \quad (9)$$

hypothesizing that X normally distributes and Y log-normally distributed and that the following relationships exist:

$$Y = e^X \quad (10.a)$$

$$X = \ln[Y] \quad (10.b)$$

Naming $\boldsymbol{Y}_i$ the i-th scalar component of the $\boldsymbol{Y}$-vector and $\boldsymbol{X}_j$ the j-th scalar component of the $\boldsymbol{X}$-vector, the scalar mean of the single components, μ_{X_i}, μ_{X_j}, the standard deviation, $\sigma_{X_i}, \sigma_{X_j}$ and the variance coefficients, $\sigma_{X_{ii}}, \sigma_{X_{jj}}, \sigma_{Y_{ii}}, \sigma_{Y_{jj}}$, of the two vectors are linked by the relationship summarized in Table 7.

Table 7: Correlation between log-normal and normal variables.

Normal to Log-Normal	Normal to Log-Normal	
$\mu_{Yi} = e^{\mu_{Xi} + \frac{1}{2}\sigma_{Xi}}$	$\mu_{Xi} = LN\left[\frac{\mu_{Yi}}{\sqrt{1+\left(\frac{\sigma_{Yi}}{\mu_{Yi}}\right)^2}}\right]$	*Mean value (11a)*
$\sigma_{Yii} = \left[e^{\sigma_{Xii}} - 1\right] \cdot e^{(2\mu_{Xi} + \sigma_{Xi})}$	$\sigma_{Xii} = LN\left[1+\left(\frac{\sigma_{Yii}}{\mu_{Yi}}\right)^2\right]$	*Standard deviation (11.b)*
$\sigma_{Yij} = \mu_{Xi}\mu_{Yi} \cdot \left(e^{\sigma_{Xii}} j1\right)$	$\sigma_{Xij} = LN\left[1+\frac{\sigma_{Yij}}{\mu_{Yj}\mu_{Yi}}\right]$	*Variance (11.c)*

Using the previous general relationships, the probabilistic models for different data set were simply obtained using a correlation matrix of observed mechanical properties:

$$R_X = \begin{vmatrix} \rho_{f_y f_y} & \rho_{f_y f_t} & \rho_{f_y A} \\ \rho_{f_t f_y} & \rho_{f_t f_t} & \rho_{f_t A} \\ \rho_{A f_y} & \rho_{A f_t} & \rho_{AA} \end{vmatrix} \quad (12)$$

where single components of the matrix are defined using following formulas and identities (13):

$$\rho_{f_y f_y} = \rho_{f_t f_t} = \rho_{AA}; \rho_{f_t f_y} = \frac{\sigma_{f_t f_y}^{\ 2}}{\sigma_{f_t}\sigma_{f_y}}; \rho_{Af_t} = \rho_{f_t A} = \frac{\sigma_{f_t A}^{\ 2}}{\sigma_{f_t}\sigma_A}; \rho_{f_y A} = \rho_{Af_y} = \frac{\sigma_{Af_y}^{\ 2}}{\sigma_A \sigma_{f_y}} \tag{13}$$

The correlation matrixes for steel materials were developed assuming the gathering of sampled data in homogeneous classes individuated by steel quality and thickness ranges. The dependence of the mechanical properties on the thickness of the plated elements was implicitly integrated in the models: different models for different thickness ranges (as individuated by EN10025:2004 and EN10219:2006). For the reinforcing bars, only one model was defined for each steel quality, neglecting the fluctuation of statistical moments due to the rebar diameter. The correlation matrix so obtained for each macro group are reported in Table 8, Table 9 and Table 10 and were used for the samples generation.

Table 8: Correlation matrix adopted for the structural steel model with thickness lower than 16 mm.

S235				S275				S355				S460			
	$R_{e,H}$	R_m	A		$R_{e,H}$	R_m	A		$R_{e,H}$	R_m	A		$R_{e,H}$	R_m	A
$R_{e,H}$	1	0,710	0,106	$R_{e,H}$	1	0,710	0,106	$R_{e,H}$	1	0,313	0,107	$R_{e,H}$	1	0,653	0,071
R_m	0,710	1	-0,092	R_m	0,710	1	-0,092	R_m	0,313	1	-0,171	R_m	0,653	1	-0,221
A	0,106	-0,092	1	A	0,106	-0,092	1	A	0,107	-0,171	1	A	0,071	-0,221	1

Table 9: Correlation matrix adopted for the structural steel model with thickness higher than 16 mm.

S235				S275				S355				S460			
	$R_{e,H}$	R_m	A		$R_{e,H}$	R_m	A		$R_{e,H}$	R_m	A		$R_{e,H}$	R_m	A
$R_{e,H}$	1	0,840	-0,298	$R_{e,H}$	1	0,736	-0,276	$R_{e,H}$	1	0,851	-0,382	$R_{e,H}$	1	0,831	-0,329
R_m	0,840	1	-0,329	R_m	0,736	1	-0,402	R_m	0,851	1	-0,577	R_m	0,831	1	-0,610
A	-0,298	-0,329	1	A	-0,276	-0,402	1	A	-0,382	-0,577	1	A	-0,329	-0,610	1

Table 10: Correlation matrix adopted for steel reinforcing bars adopted in composite structures.

B500B			
	$R_{e,H}$	R_m	A
$R_{e,H}$	1	0,908	-0,542
R_m	0,908	1	-0,431
A	-0,542	-0,431	1

The procedure adopted for generating samples was organised according to the following steps:

- transformation of mean, variance and co-variance, μ_{yi}, σ_{yi} and σ_{yii}, associated to Log-Normal distribution into the corresponding mean, variance and co-variance, μ_{xi}, σ_{xi} and σ_{xii}, associated to an equivalent Normal distribution using relationships in Table 7;
- definition of probability density function and correlation matrix:

$$R_X = E\left[(X - \mu_X)(X - \mu_X)^T\right] \tag{14.a}$$

$$f_X = \frac{1}{(2\pi)^{N/2}\sqrt{\|R_X\|}} e^{\left[-\frac{1}{2}(X-\mu_X)^T R_X^{-1}(X-\mu_X)\right]} \tag{14.b}$$

- generation of mechanical variable samples adopting a Monte Carlo approach;
- transformation of generated samples in the Log-Normal distributed variables using the relationships of Table 7.

4.3 *Uni-axial constitutive law for steel*

In order to complete the characterization of steel products, on the basis of a database of about 60 curves collected by industrial partners from profiles of different qualities (including S235, S375 and S355), an appropriate monotonic-skeleton curve for steel stress-strain law was then elaborated. The model was validated comparing results with an experimental cyclic testing executed on a steel beam (Schäfer et al. 2010).The analysis of the experimental stress-strain curves identified 4 significant points (Figure 3):

- point P1 – the yielding point in which $R_{e,H}$ and ε_y are localized.
- point P2 – the end of the yielding plateau in which $f_h = R_{e,H}$ and ε_h are localized.

- point P3 – the point at which the maximum load is reached where f_t=R_m and A_{gt} are localized.
- point P4 – the elongation at fracture ε_u and corresponding strength $f(\varepsilon_u)$.

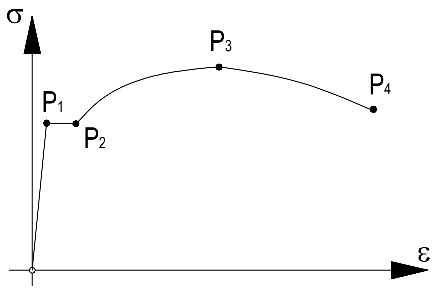

	x	y
O	0	0
P1	ε_y	f_y
P2	ε_h	f_h
P3	A_{gt}	f_t
P4	ε_u	$f(\varepsilon_u)$

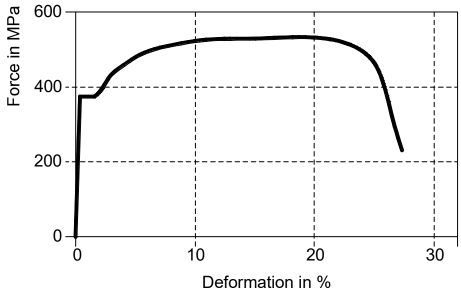

Figure 3: Stress strain law of steel profiles: a) monitored points; b) experimental curve taken from collected database.

The experimental values related to the described four points were statistically analyzed correlating P2 and P3 values with the three mechanical parameters assumed as probabilistic variables in the present study: f_y ($R_{e,H}$), f_t (R_m) and ε_u (A_{gt}). To these purposes, a linear regression was executed in order to correlate ε_h and ε_t with the three variables and thus having the stress-strain law as function of f_y, f_t and ε_u. The formula (15) shows the linear relationships adopted for linear regression whose parameters are presented in Table 11. In Figure 4 the comparison between experimental data and values evaluated by the model are shown.

$$\begin{aligned} \varepsilon_h\left(f_y, f_u, \varepsilon_u, t\right) &= A_0 + A_1 \cdot f_y + A_2 \cdot f_u + A_3 \cdot \varepsilon_u + A_4 \cdot t \\ \varepsilon_t\left(f_y, f_u, \varepsilon_u, t\right) &= B_0 + B_1 \cdot f_y + B_2 \cdot f_u + B_3 \cdot \varepsilon_u + B_4 \cdot t \end{aligned} \qquad (15)$$

Table 11: Formulas obtained from multi-linear regression form experimental data recorded during the tensile testings.

A0	7,10E-02	B0	3,60E-01
A1	1,40E-04	B1	-4,90E-04
A2	-1,70E-04	B2	9,60E-05
A3	-4,10E-02	B3	-1,40E-01
A4	-3,30E-04	B4	-1,10E-03

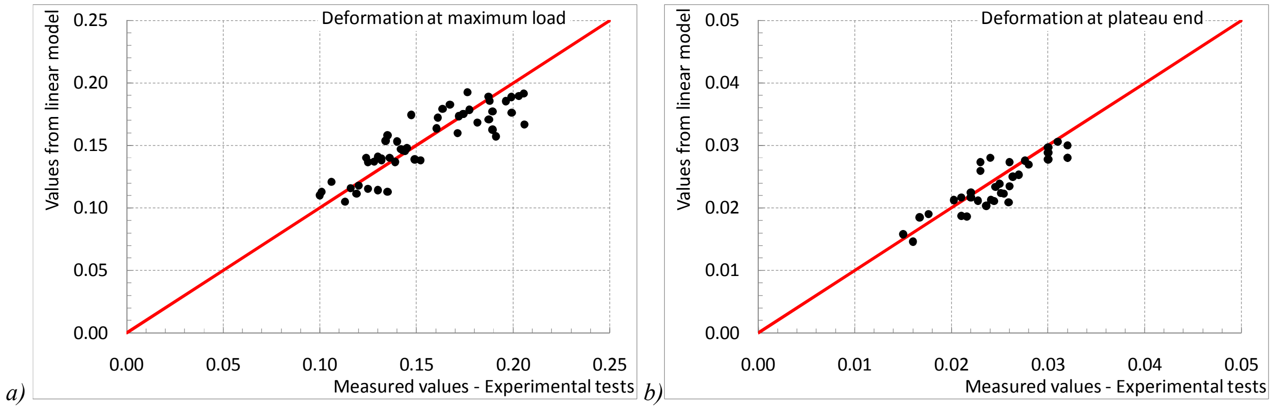

Figure 4: Relation between the measured values and predicted values for: elongation at maximum load and at plateau-end.

Validation of regression data and of the obtained stress-strain laws was made against the experimental results obtained in Schäfer et al. (2010). More details and information on validation can be found in Braconi et al. (2013b). Basing on such calibration, for sake of simplicity, a model including kinematic hardening, was chosen in the present study.

5. Modelling of the seismic hazard

5.1 European Seismic Hazard and Seismic Input

According to EN1998-1:2005, the annual rate of exceedance of the reference peak ground acceleration (PGA) is expressed by the following relationship (16):

$$H\left(a_{gR}\right) = k_0 \cdot PGA^{-k} \qquad (16)$$

where the factor k - related to seismicity of the area- is usually assumed equal to 3 as representative of the European region. The value of k_0 is fixed according to the basic performance requirements in order to fit general requirements of seismic action for the Non Collapse Requirement (NCR). The seismic action assumed during the structural design was then characterized by an exceeding probability of 10% (P_{NCR} - probability of Non Collapse Requirement) in 50 years (T_L - exposition or reference period of the structure). The return period of seismic action (T_R), correlated with P_{NCR} and T_L, was then equal to 475 years for the design PGA associated to NCR.
During the design of selected case studies, PGA respectively equal to 0.25g and 0.10/0.15 g were selected for high and low seismic regions, associated to a rigid soil (typology "A" with $V_{S,30}$ higher than 800 m/s) and to a unitary importance factor (γ_I). The importance factor can be increased accordingly to classification proposed by National Authorities for each seismic zone and the design PGA through following relation (17):

$$PGA_{adopted} = \gamma_I \cdot PGA \tag{17}$$

Different PGA levels were associated to the relevant Limit States, which were grouped in two macro-groups: damage limitation group and collapse prevention group.
The level of seismic action corresponding to the absence of damage (i.e. complete integrity of infill walls or partition walls) was determined scaling the design seismic action in order to taking into account a lower return period by using ν parameter as proposed by EN1998-1:2005. The parameters of the hazard function fixed assuming the reference k factor proposed by Eurocode 8 (EN1998-1:2005) and imposing the correspondence between PGA levels and appropriate limit states are listed in the Table 12.

Table 12: Levels of PGA with the corresponding return period and exceedance threshold probability for high and low seismicity areas and parameters calibrated according to chosen PGA design levels.

	Limit State	T_R	$P_{exceedance}$		High seism. PGA	Low seism. PGA	$PGA_{LS/IO}$	k and k_0 factors			
			T_L=50 y	T_L=1 y			ν factor		T_L=1 y	k	3
		[years]	[%]	[%]	[g]	[g]	[-]	High Seismicity		k_0	3,32E-05
Damage Limitation Requirement	IO	30	81	3,27	0,10	0,04	0,40		T_L=50 y	k	2,28
	DL	50	63	1,97	0,12	0,05	0,47			k_0	4,22E-03
	DL	95	41	1,05	0,15	0,06	0,58	Low Seismicity	T_L=1 y	k	3
No Collapse Requirement	LS	475	10	0,21	0,25	0,10	1,00			k_0	2,14E-06
	CP	975	5	0,10	0,32	0,13	1,27		T_L=50 y	k	2,28
	CP	2475	2	0,04	0,43	0,17	1,74			k_0	5,21E-04

5.2 Generation of the seismic inputs

Seven artificially generated and statistically independent time histories were generated from the design spectra using the SIMQKE software (Vanmarcke et al. 1999).The parameters reported in Table 13 were used for generating the artificial earthquakes (PGA, spectrum type and soil) at which a trapezoidal filtering function (total and strong motion duration) was applied. The relevant eigen-periods were assumed to be in a range between 0.1 s and 3.0 s. The chosen sampling interval of $\Delta t = 0.01$ s allowed a sufficient accurate calculation for eigen-frequencies up to 20Hz (5 points for each period); more details can be found in the Opus final report (Braconi et al. 2013b), Braconi et al. (2015) and Badalassi et al. (2015). For each type of seismic intensity (design spectrum), 7 artificial accelerograms were generated.

Table 13: Parameters of target spectra and filter function for low and high seismicity.

Seismicity	PGA	spectrum	soil	total duration	strong motion duration
Low	0.10 g	Type 2	Type C	15 s	5 s
High	0.25 g	Type 1	Type B	20 s	10 s

A baseline correction was applied to the accelerograms in order to avoid displacements running outland so obtaining a sufficiently small displacement at the end of the record (Badalassi et al. 2013). The adequacy of the accelerograms was checked through the evaluation of the related elastic response spectra (Figure 5). For periods lower than T_B the spectral value S_a resulted slightly high, however the requirements defined in EN19981:2005 were fulfilled. The COV of the spectral values for the 7 accelerograms was between 0.04 and 0.12 (Braconi et al. 2013b).

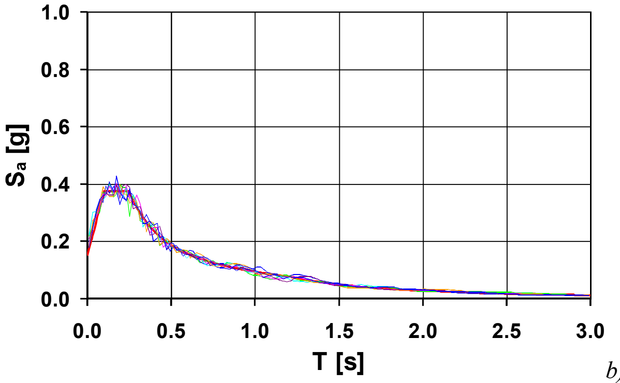

a)

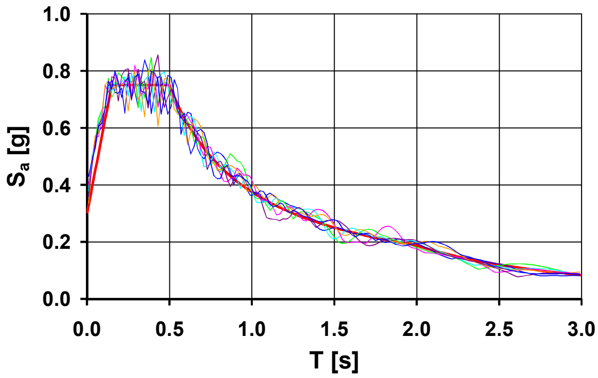

b)

Figure 5: Target spectrum and elastic response spectra of 7 artificial accelerograms: a) low and b) high seismicity.

6. IDA and application of probabilistic procedures

In general, the estimation of exceeding a certain limit state (i.e. missing an expected performance) within a given period can be calculated adopting the general probabilistic approach proposed by Pacific Earthquake Engineering Research centre (Porter 2003) summarized as:

$$\lambda(DM) = \iint G(DM|EDP) \cdot |dG(EDP|IM)| \cdot |d\lambda(IM)| \tag{18}$$

where λ(EDP) is the annual probability of exceedance of EDP of a fixed limit.
The variables involved in the equation are:

- Intensity Measure (IM). This denotes the ground motion intensity through an appropriate measuring scale as for instance, PGA or the spectral acceleration $S_{e,PGA}(T_0)$.
- Engineering Demand Parameters (EDPs). The seismic demand needs to be characterized by a set of response measures –EDPs – as for instance, top roof displacement, interstorey drift ratio or others that can be correlated with damage and performance of the facility.
- Damage Measures (DMs). This refers to the conversion of response measures to quantifiable damage states that can be identified after the seismic event and correlated to facility performance.

The output of IDA simulations defines the correlations between EDP and IM by collapse criteria of the structural system that relate DMs to EDPs. The different terms contained in (18) have the following role:

- $G(DM|EDP)$ is the complementary cumulative distribution function or the conditional probability that DM exceeds a specific limit value given a set of EDPs;
- $|dG(EDP|IM)|$ is the probability density function that EDPs exceeds a specific response threshold given the intensity level of the earthquake (i.e. the fragility of the facility);
- $|d\lambda(IM)|$ is the differential of the mean annual frequency of exceeding the intensity measure (which for small values is equal to the annual probability of exceedance of the intensity measure).

The PEER framework can be further specified taking into account the variability of mechanical properties as well through the following formulation:

$$\lambda(DM) = \iint G(DM|EDP) \cdot |dG(EDP|IM, MV)| \cdot |d\lambda(MV)| \cdot |d\lambda(IM)| \tag{19}$$

where the material variability (MV) is explicitly considered in the formulation of annual exceedance probability $\lambda(DM)$. The term $G(EDP|IM, MV)$ refers to the structural response, i.e. the cumulative density function of the probability that EDPs exceed a certain threshold given an IM level and a set of material properties MV. The equation (19) is numerically estimated using the IDA outputs being extremely complex solving the PEER approaches in a closed form, especially with complex facilities.

6.1 Performing of the IDAs within the PEER framework

The IDA simulations carried out in the present work (7 earthquake × 500 set of mechanical properties × N PGA levels) directly integrated the variability of IM and MV into the EDP, resulting in the fragility for a given intensity and material variability of each relevant collapse mode of the structure under examination. Then the fragility was integrated with the seismic hazard associating the probability of failure for each relevant collapse mode of the case study to the specificities of the site. In such a case, the result of the analysis is expressed in the annual probability of exceeding a given threshold of the response given a specific IM of the site.

Concerning the variability of the mechanical properties, it was assumed as probabilistically independent for beams and columns whereas the columns of two subsequent floors were assumed as totally correlated (e.g. steel from the same heat). Moreover, the PGA levels to be explored during each IDA procedure were preliminary identified for using only those activating the relevant collapse criteria for each case study; therefore strip method approach for the simulations were applied (Pinto et al. 2004).
The IDA output was standardized (standardised variables), defining auxiliary variables, one for each collapse criterion, dividing the i-th component of EDP – EDP_i – by the correspondent value identifying the exceedance of a limit state – $DM_{i,u}$:

$$Y_i = 100 \cdot EDP_i / DM_{i,u} \tag{20}$$

These standardised variables were analysed for evaluating the basic statistical parameters and tested against the χ^2 test for identifying a suitable statistical distribution. When the test was not negative, a Normal or Log-Normal distribution was assumed. Instead, with a negative test, the statistical cumulative density function was numerically built directly from data and completed with tails built up using exponential functions calibrated through the IDA output.
The probability of failure for each collapse criterion associate to a PGA level and an accelerogram was evaluated using its cumulative density function, being $P_f = P[Y > 100]$, calculated as the average fragility curve of each specific collapse criterion (Figure 6).

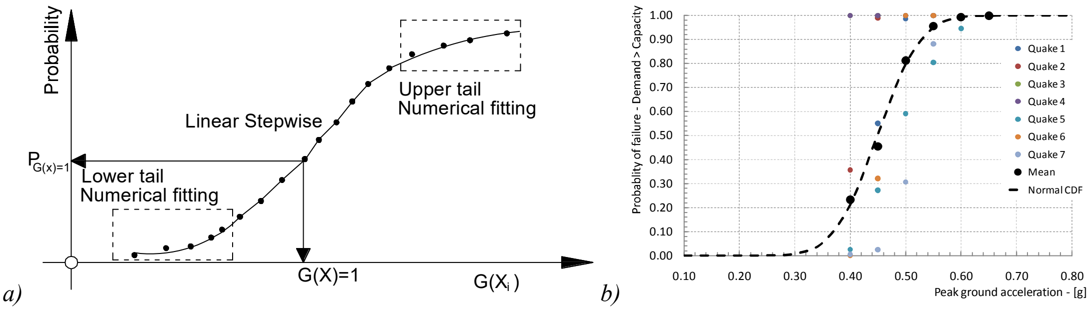

Figure 6: a) Numerical CDF derived from IDA results (χ^2 failed); b) fragility of 3EBFX for ultimate plastic rotation of link B1.

7. Exploitation of IDA results

7.1 Probabilistic assessment of structural performance

The probabilistic procedure was first applied for estimating the reference P_{fail} characterised by the variability of the material mechanical properties (500 samples) considering 7 seismic input (7 artificial accelerograms compatible with the design spectrum). Subsequently, the P_{fail} was re-evaluated using a set of pre-conditioned samples in order to simulate the application of an additional quality check to the EN10025:2004 requirements (for instance, the requirements imposed by EN1998-1:2005 to structural steels).
The 500 samples generated for each structural case study were reduced imposing that the steel properties in the dissipative zones had a fixed maximum yielding stress ($f_{y,act}$), Figure 7, as foreseen by EN1998-1:2005 where $f_{y,act}/f_{y,nom}$=1.25. The numerousness of reduced samples set was different for each case study due to the randomness of Monte Carlo generation of the samples (i.e. steel quality variability), not allowing to entirely carry out the same analysis for all the case studies.
In the following, the results of probabilistic analyses are presented grouping the case studies considering the structural typology, as follows:

- Steel EBF buildings (n°3, 4 and 16).
- Composite steel-concrete buildings (n°6, 7, 8, 9, 10 and 11).
- Buildings with combined MRF and CBF (or EBF) structure (n°1, 2, 5, 13, 14 and 15).

The reference P_{fail} was assumed as represented by the structural safety attainable adopting EN1998-1:2005 design procedure and the EN10025–1÷6 (2004) production standard as actually issued by CEN. Its variation was then estimated referring to the upper limitation of yielding stress.
The analysis of P_{fail} values was performed assuming that a value of 10^{-3}, i.e. yearly failure probability associated to seismic action return period of 475 years, is acceptable failure probability of a single structural member (Melchers 2002, Hasofer et al. 1974, Ellingwood et al. 1980, Porter et al. 1998) belonging to the case studies (whose design was optimized).

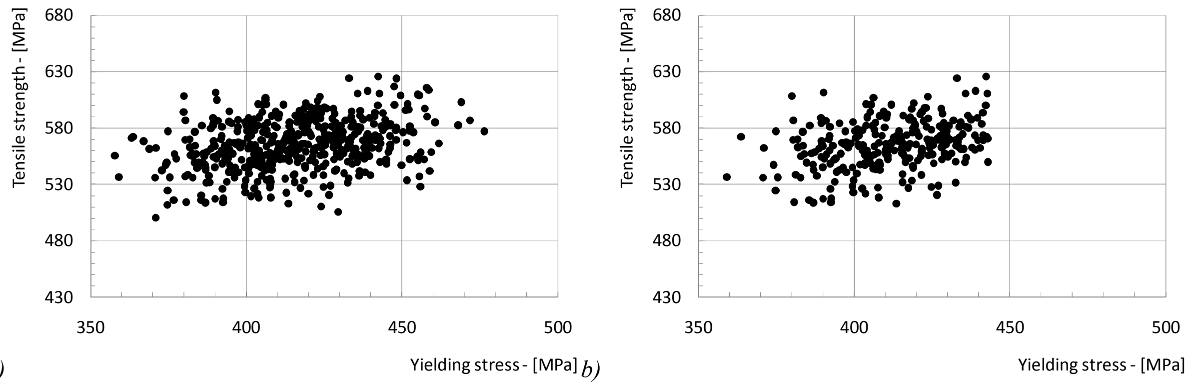

Figure 7: Samples for link B1 in the 3EBFX: a) 500 samples EN10025 full generation, b) reduced number imposing $f_{y,act}/f_{y,nom}$=1.25

7.2 Results of probabilistic investigations

In the following paragraphs the estimated P_{fail} of the different case studies are presented. The tables show the results related to the structural elements for which the relevant collapse criteria activate or for which the estimated probability is not extremely low, in relation to the different structural typologies considered.

7.2.1 EBF resisting system – Case 3, 4 and 16.

The case study n°3 (Figure 8.a) showed a P_{fail} of the braces (criteria G; Br1, Br2, Table 14) lower than those along Y direction (criteria G; Br1, Br2) due to the limitation of lateral displacements required by frame 3X configuration compared to frame 3Y. The design of the links was accurate in both frames and aimed at optimizing Ω factors and avoiding oversized seismic links: this resulted in comparable values of P_{fail} (Criteria N; 3X: B1-5; 3Y: B1-20). P_{fail} of the first story columns was very low due to the highest demand imposed by the static load combination (Criteria G; 3X: collapse not activated at all; 3EBFY: C1, 2 and 4).

The design of case n°4 (Figure 8.b) resulted in an estimation of the P_{fail} generally lower than the values in the case n°3 (around one order of magnitude, Table 15). This is a consequence of the design requirements (low seismic hazard and lower ductility) and the adopted seismic design procedure that yielded oversized structural elements.

The case study n°16 (Figure 8.c) due to its geometry showed values of the estimated P_{fail} similar to those shown by case 3 for the seismic links (criteria N; 16X: B1-B6, 16Y: B1-B12, Table 16), the braces (criteria G, 16X: Br1-Br6; 16Y: Br1-Br6) and the columns (criteria G; 16X: C1-C4; 16Y: C1-C7). Values of annual probability of failure were in-line with the limit proposed by Melchers (2002), equal to 10^{-3}under seismic actions. Eurocode capacity design approach - material over-strength factor, γ_{OV}, and structural over-strength, Ω - ensures an adequate protection level and in some cases leaded to very conservative design.

The probabilistic procedure was then newly applied imposing a preconditioning of material input variables: the real yielding value of steel quality – $f_{y,act}$ – used in the dissipative members was limited imposing different upper limits (fictitious production controls) equal to 1.375, 1.35, 1.30 and 1.25 times the nominal yielding – f_y. The introduction of these controls reduced the numerousness of the materials sample to be used in the probabilistic procedure: the reduction was less evident for S355 quality than for S275 quality.

The effects of these fictitious production controls on case n°3 and case n°4 are shown in Figure 9 and Figure 10. It is worth noting the larger effects of the control on the case 4 – made using S275 – than the effects on case n°3 – made on S355, whose quality production controls are expected to be tighter. In general, the introduction of "production control" caused a variation in the estimated risk: the variation of link failure goes from +2% to +25% while the variation of the brace failure goes from -1% to -35%. It is thus undeniable that stricter the production control, larger the demand on ductile elements of the structural system: therefore, the threshold of the $f_{y,act}$ fixed by production controls should be thoroughly weighed in order to avoid unbalanced solution in which the exploitation of plastic resources might be excessive.

In the cases of the bracing elements, Figures 9.b and 10.b, the braces less conditioned by stiffness requirements showed the larger decrements in failure probability, while those over-sized by the designing process were not influenced by "production controls".

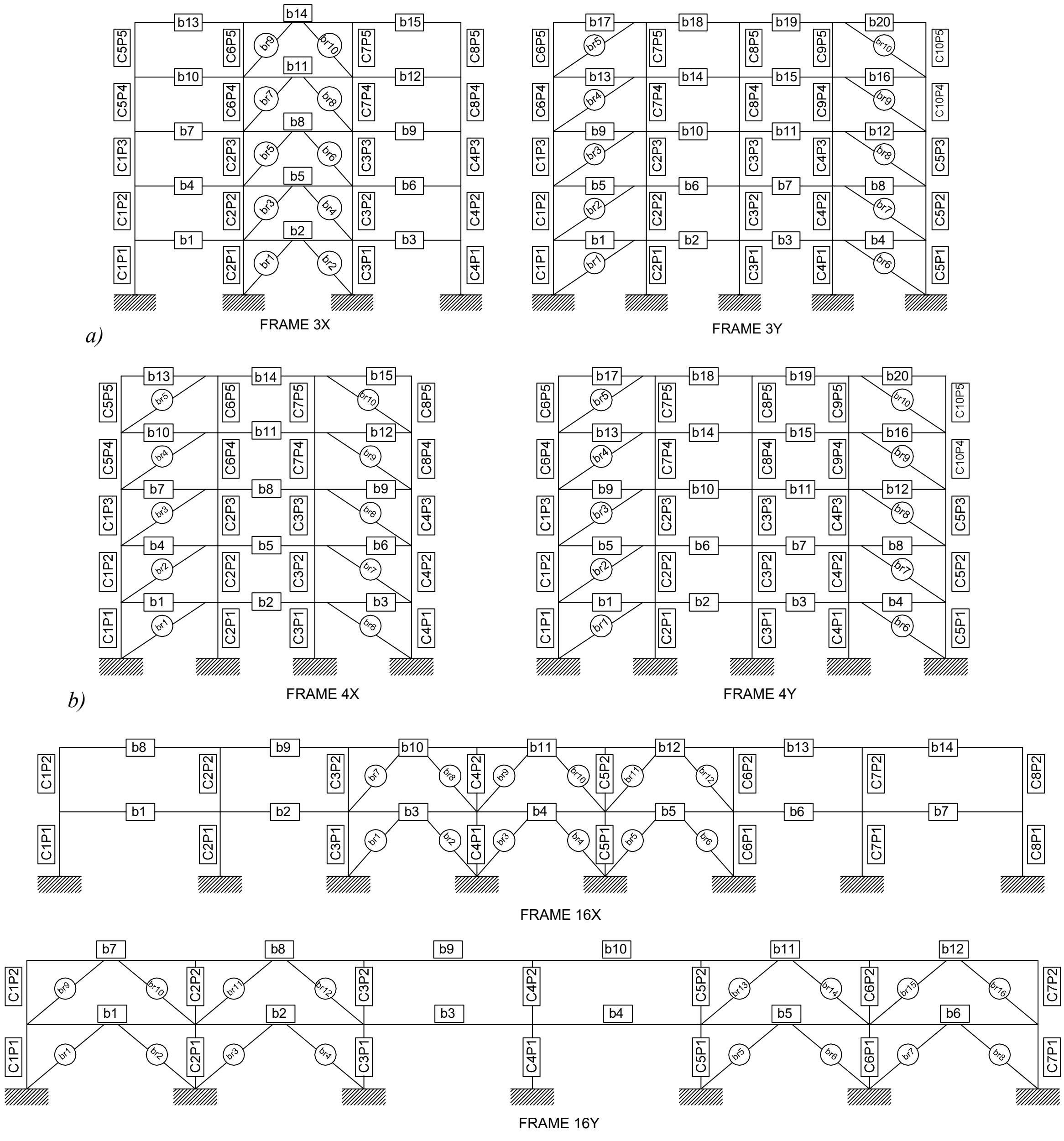

Figure 8: a) Frame 3 with EB resisting scheme with shear links in X and Y directions; b) Frame 4 with EB resisting scheme with bending links in X and Y directions, c) Frame 16 with EB resisting scheme with shear links in X and Y directions.

Table 14: Annual exceedance probability (Seismic risks) associated to building ID n°3 (EBF) collapse modes.

Building ID n°3 – X direction							
Element	B1	B2	B3	B4	B5	Br1	Br2
$P_{f,N}$	4.10E-04	4.20E-04	4.10E-04	2.80E-04	2.00E-04	4.50E-05	4.30E-05
Element	Drift 1	Drift 2	Drift 3	Drift 4	Drift 5		
$P_{f,N}$	2.80E-04	3.00E-04	1.60E-04	1.00E-04	9.30E-05		
Building ID n°3 – Y direction							
Element	B1	B4	B5	B8	B9	B12	B13
$P_{f,N}$	2.90E-04	3.10E-04	9.30E-05	1.30E-04	8.80E-05	1.30E-04	5.70E-05
Element	B16	B17	B20	Drift 1	Drift 2	Drift 3	Drift 4
$P_{f,N}$	8.20E-05	3.60E-05	5.3-05	2.80E-04	7.10E-05	5.30E-05	3.30E-08
Element	Drift 5	Br1	Br2	C1	C2	C4	
$P_{f,N}$	3.30E-08	2.80E-04	2.40E-04	1.50E-06	5.90E-06	1.50E-06	

Table 15: Annual exceedance probability (Seismic risks) associated to building ID n°4 (EBF) collapse modes.

Building ID n°4 – X direction							
Element	B1	B3	B4	B6	B7	B9	B10
$P_{f,N}$	1.20E-05	1.10E-05	3.80E-06	3.70E-06	1.10E-06	9.60E-07	1.10E-07
Element	B12	B13	B15	Drift 1	Drift 2	Drift 3	Drift 4
$P_{f,N}$	3.50E-07	8.30E-06	9.50E-06	5.50E-06	1.70E-07	4.20E-09	5.50E-08
Element	Drift 5	Br1	Br2	C1	C2	C3	C4
$P_{f,N}$	5.50E-08	1.10E-05	1.00E-05	2.40E-15	2.00E-14	2.40E-15	2.40E-15
Building ID n°4 – Y direction							
Element	B1	B4	B5	B8	B9	B12	B13
$P_{f,N}$	1.20E-05	1.30E-05	2.70E-06	2.80E-06	4.20E-07	4.40E-07	2.00E-06
Element	B16	B17	B20	Drift 1	Drift 2	Br1	Br2
$P_{f,N}$	2.40E-06	2.30E-02	2.90E-02	4.50E-06	1.30E-06	1.20E-05	2.30E-05

Table 16: Annual exceedance probability (Seismic risks) associated to building ID n°16 (EBF) collapse modes.

Building ID n°16 – X direction							
Element	B1	B2	B3	B4	B5	B6	Br1
$P_{f,N}$	1.90E-04	2.00E-04	2.10E-04	3.40E-05	3.60E-05	3.40E-05	1.60E-04
Element	Br2	Br3	Br4	Br5	Br6	Drift 1	Drift 2
$P_{f,N}$	1.50E-04	1.50E-04	1.50E-04	1.60E-04	1.60E-04	2.40E-04	3.90E-05
Element	C1	C2	C3	C4			
$P_{f,N}$	3.50E-06	1.50E-05	1.50E-05	4.50E-06			
Building ID n°16 – Y direction							
Element	B1	B2	B5	B6	B7	B8	B11
$P_{f,N}$	2.60E-04	2.60E-04	2.60E-04	2.60E-04	3.60E-06	3.6E-0603.6E-06	
Element	B12	Br1	Br2	Br3	Br4	Br6	
$P_{f,N}$	3.60E-06	5.00E-06	5.10E-06	9.80E-06	5.40E-06	4.70E-06	
Element	C1	C2	C3	C5	C6	C7	
$P_{f,N}$	7.60E-08	7.60E-08	7.60E-08	7.60E-08	3.00E-07	3.00E-07	

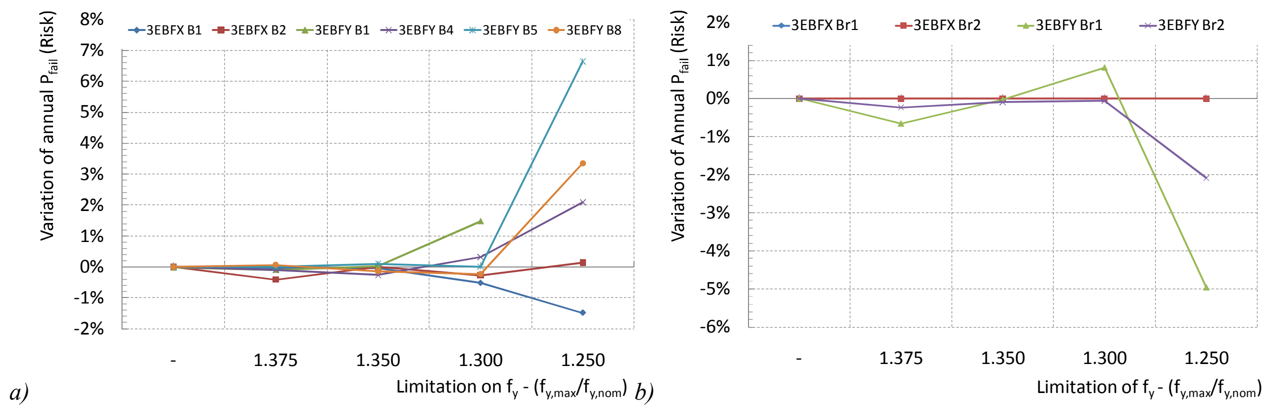

Figure 9: a) variation of P_f -ultimate plastic rotation of links – 3EBF; b) variation of P_f for buckling of first storey braces – 3EBF.

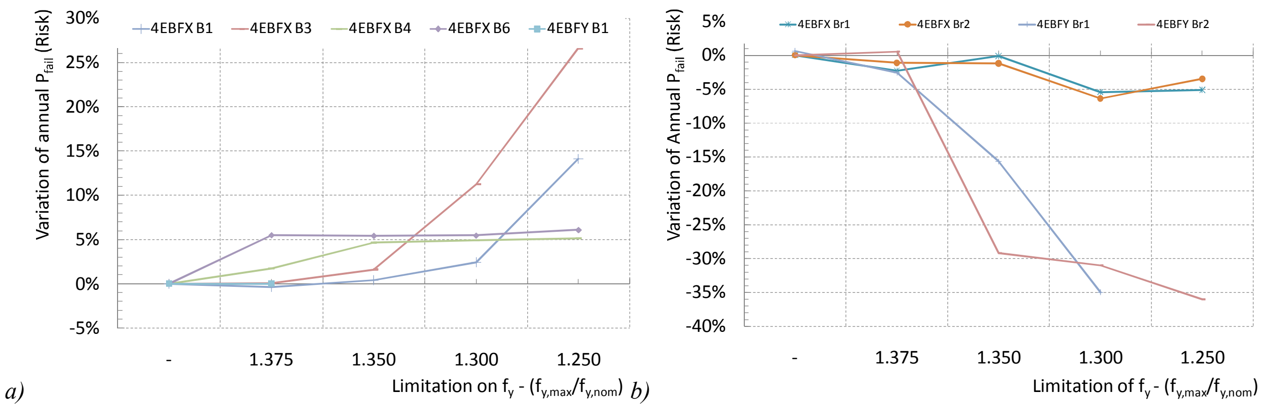

Figure 10: a) variation of P_f- ultimate plastic rotation of links – 4EBF; b) variation of P_f- buckling of first storey braces – 4EBF.

7.2.2 Steel-Concrete composite resisting system – Case 6, 7, 8, 9, 10 and 11.

In the case of braced steel-concrete composite frames (i.e. buildings n°10 and n°11 – EBF resisting system was adopted in X direction and CBF resisting system in Y direction - Figure 11), the unique collapse criteria activated by different earthquakes were the ultimate deformation of shear links and the maximum elongation of concentric braces. The probabilistic procedure and the effects introduced by the "fictitious production controls" thus applied only to the most solicited shear link and the most solicited brace elements: the shear link located at the top story of the EBF configuration (Link5 – Figure 11.a) and the brace located at the lower storey, the left diagonal (diag1L – Figure 11.b) of the CBF configuration.

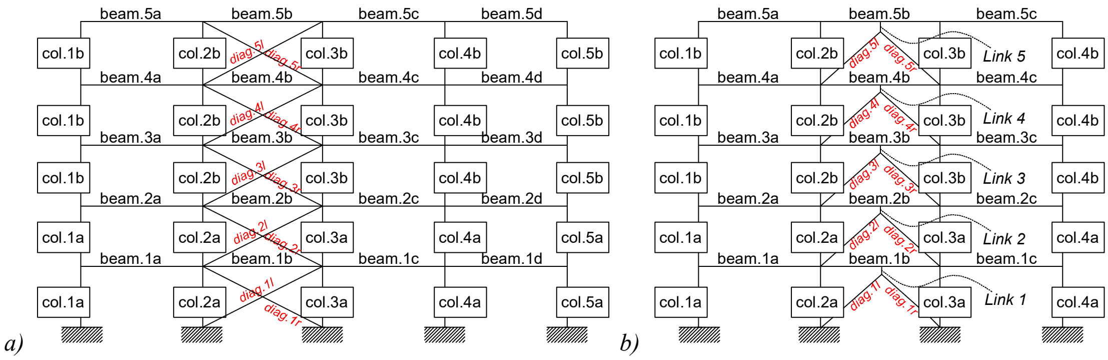

Figure 11: a) Building 10 – EBF configuration, b) Building 11 – CBF configuration.

The estimated failure probability of the cases n°10 and n°11 was lower than values usually suggested by the literature (Table 17). Moreover, the additional production controls on the adopted steel qualities did not substantially modified the estimated failure probability not showing a clear trend as that identified in the cases 3 and 4 for which the design procedure led to a more optimised solution.

Table 17: Yearly probability associated to active collapse criteria with different upper limitations to yielding.

		High Seismicity	Low Seismicity	High Seismicity	Low Seismicity
	Element	Diag1L	Diag1L	LinkS5	LinkS5
No f_y limit	Seismic Risk	6,41E-05	3,95E-06	2,29E-05	5,60E-06
$f_{y,max}$<1.375$f_{y,nom}$	Seismic Risk	6,42E-05	3,79E-06	2,29E-05	4,16E-06
$f_{y,max}$<1.30$f_{y,nom}$	Seismic Risk	5,91E-05	3,66E-06	2,28E-05	3,15E-06
$f_{y,max}$<1.25$f_{y,nom}$	Seismic Risk	6,64E-05	-	2,28E-05	4,63E-06

The cases 6, 7, 8 and 9 were related to MRF resisting systems whose configuration is showed in Figure 12.a: their design was carried out assuming rigid connections and joints. These design assumptions and the adopted designing procedure gave as unique activated collapse criteria the ultimate rotation of plastic hinges. In particular, the probabilistic procedure focused on the elements 1 – column base – and 12– beam – (Figure 12.a), being the most solicited members. The results are reported Table 18. In this case, the influence of variability of seismic action and of material mechanical properties was not so high to endanger the structural safety respect with relevant collapse modes. Moreover, the introduction of the additional quality control on the steel produced according to EN10025:2004 did not produce appreciable variations of the failure probability of the collapse criteria, Figure 12.b, caused, on the contrary, mainly by the presence of the concrete. However, it is worth underlining that the adoption of steel-concrete solutions instead of the bare steel one for the columns guaranteed lower values of probability of failure associated to the plastic hinge rotation at the base of the columns.

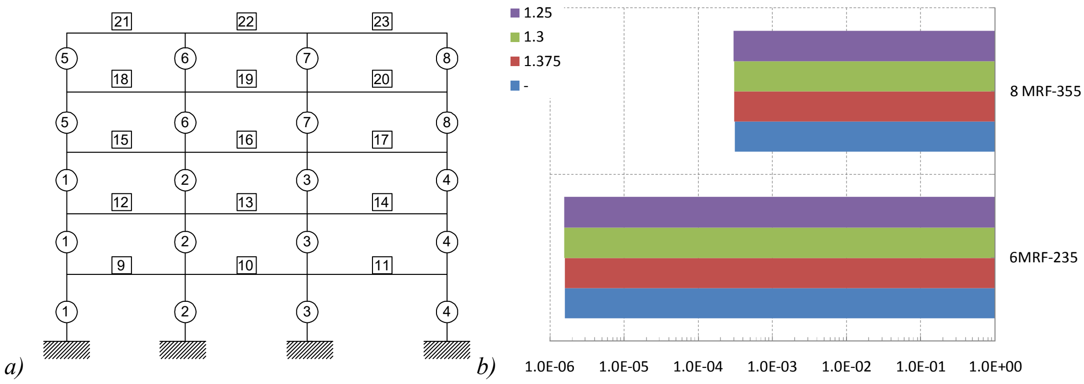

Figure 12: a) ID of structural members inside composite steel-concrete MRF (6, 7, 8 and 9), b) Influence of upper yielding limits on the P_f for ultimate plastic hinge rotation of Column 1: case 6 composite columns; case 8 bare steel columns.

Table 18: P_f estimated for the ultimate rotation of plastic hinges.

	6 MRF		7 MRF		8 MRF		9 MRF	
Element	1	12	1	12	1	12	1	12
Seismic Risk	1,83E-05	1,60E-06	1,41E-05	1,82E-04	2,68E-04	3,11E-04	1,35E-04	7,16E-3

7.2.3 MRF and CBF steel resisting system – Case 1, 2, 5, 12, 13, 14 and 15.

Cases 1, 2, 5, 12, 13, 14 and 15 were constituted by combined MRF/CBF resisting systems in the two main directions of the structures. ID numbers of the structural members of the analysed structures are shown in Figure 13, Figure 14, Figure 15 and Figure 16. In the case of steel buildings 5, 12 and 13, the structural members subjected to the probabilistic investigation were the bracings at the ground floor (braces 10, 11 – Case 5 – and brace 4 – Case 13), the columns at the ground floor (columns 3 and 5 – Case 5 – columns 1 and 5 – Case 12 – columns 1, 3 and 5 – Case 13) and the main beams of the two bays industrial building. The estimated probability of failure, reported in Tables 19-21, indicated an extremely high safety level for structures designed according to the EN1998-1:2005, if compared with the safety levels usually suggested in the literature. Moreover, the adoption of higher steel quality produced higher safety level for the collapse mode associated to column buckling while for the bracing members variation of probability of failure was less evident or negligible. Unfortunately, the mechanical properties samples generated for Cases 5, 12 and 13 did not allow applying the "fictitious production controls" because imposing an upper limit to the yielding strength even minimum, as $1,375\times f_{y,nom}$, did not leave enough material samples to apply the probabilistic procedure.

Table 19: Estimated P_f for the buckling of more solicited braces.

	Braces								
	5 CBF S355		5 CBF S460		13 CBF S235		13 CBF S275		
Element	Brace 10	Brace 11	Brace 10	Brace 11	4 - compr	4 - tens	4 - compr	4 - tens	
Seismic Risk	2,35E-08	2,32E-08	2,04E-08	3,42E-08	4,43E-08	1,81E-08	2,87E-08	2,92E-08	
	Column Buckling								
	5 MRFX S355		5 MRFX S460		12 CBF S355		13 MRFX S235		
Element	3bottom	5bottom	3bottom	5bottom	1	5	3bottom	1bottom	5bottom
Seismic Risk	2,43E-05	2,81E-03	4,91E-06	1,22E-04	1,20E-08	1,19E-08	1,28E-07	1,16E-08	1,49E-06

Table 20: P_f estimated for the buckling of more solicited columns and braces.

	Braces							
	5 CBF S355		5 CBF S460		13 CBF S235		13 CBF S275	
Element	Brace 10	Brace 11	Brace 10	Brace 11	4 - compr	4 - tens	4 - compr	4 - tens
Seismic Risk	2,35E-08	2,32E-08	2,04E-08	3,42E-08	4,43E-08	1,81E-08	2,87E-08	2,92E-08

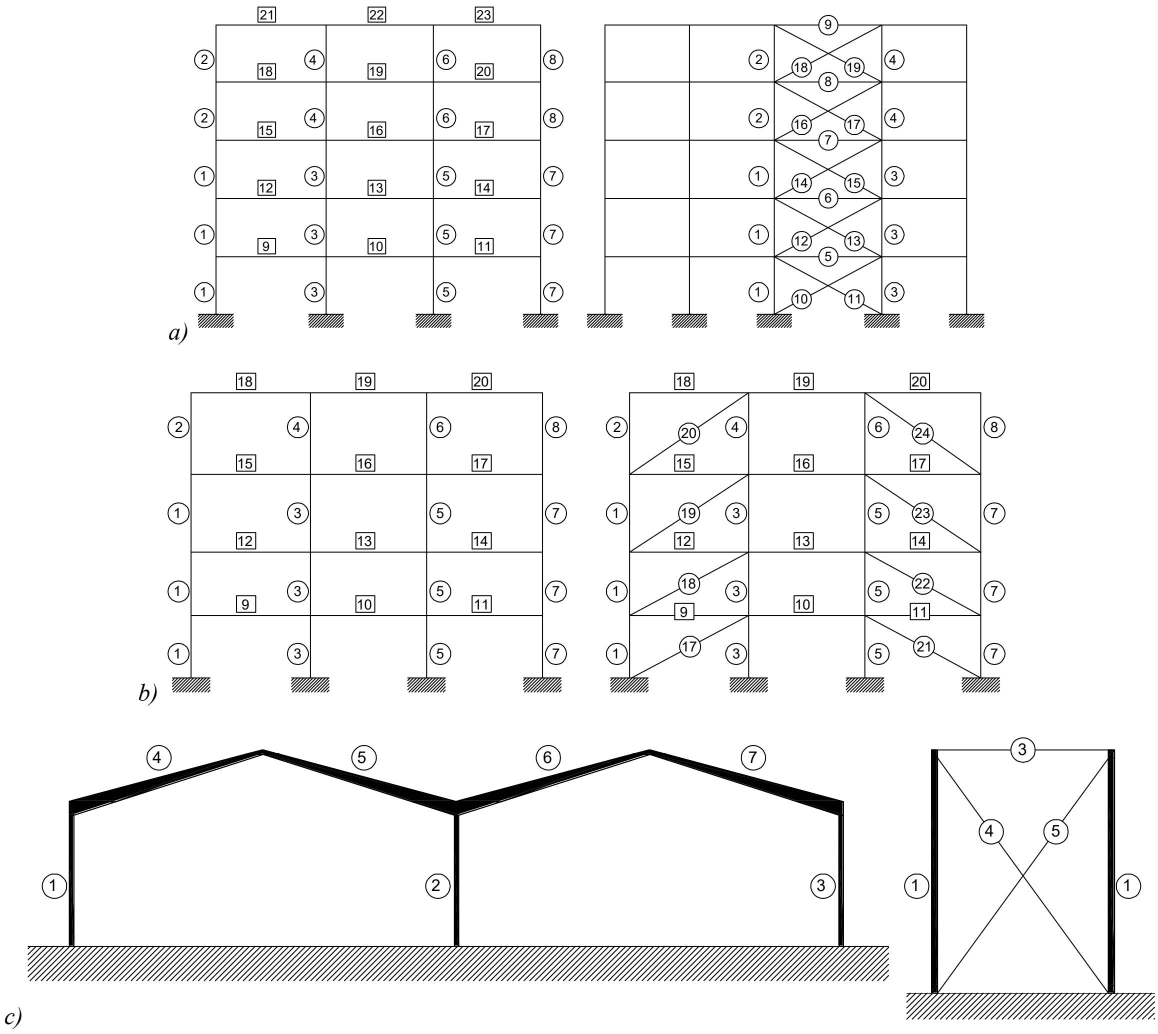

Figure 13: Identification of members analysed with probabilistic procedure of: a) Frame 5, b) Frame 12, c) Frame 13.

The entire probabilistic procedure, considering the "fictitious production controls" as well, was applied to the industrial buildings 14 and 15 and to the office buildings 1 and 2 on the more solicited elements for which the relevant collapse criteria can be activated: columns 3 and 5 of Case 1; columns 1 and 3 of Case 14; Columns 3 and 5 and Braces 24 and 28 of Case 15; braces 28 and 33 of Case 2 (see Figures 15, 16 and 17). The collapse mode of the columns was the ultimate rotation of plastic hinge whereas the collapse criterion of the braces was the ultimate elongation in tension.

Table 21: Estimated P_f for the exhaustion of rotational capacity of more critical plastic hinges and for the steel braces in tension.

	1 MRFX S235		14 MRFX S355		15 MRFX S355		2 CBFX S235		15 CBFY S355	
Element	3a-bot	5a-bot	1-bot	3-bot	3a-top	5a-top	28	33	24	28
Seismic Risk	2,2E-06	2,2E-06	1,9E-04	2,0E-04	8,7E-07	8,6E-07	9,0E-06	5,2E-06	3, 7E-04	2,4E-04

The probability of failure associated to the relevant collapse criteria was, in all cases, in-line with the safety limit usually accepted in structural safety under seismic actions. The variability of mechanical properties was completely covered by capacity design approach as for all the other cases previously analysed.

The introduction of the "fictitious production controls" induced a premature plasticization of dissipative zones so causing a moderate increase of the failure probability associated to ductile failure modes (Table 22). Anyway, from a quantitative point of view, the influence of upper yielding limitation was very limited as in all the other cases.

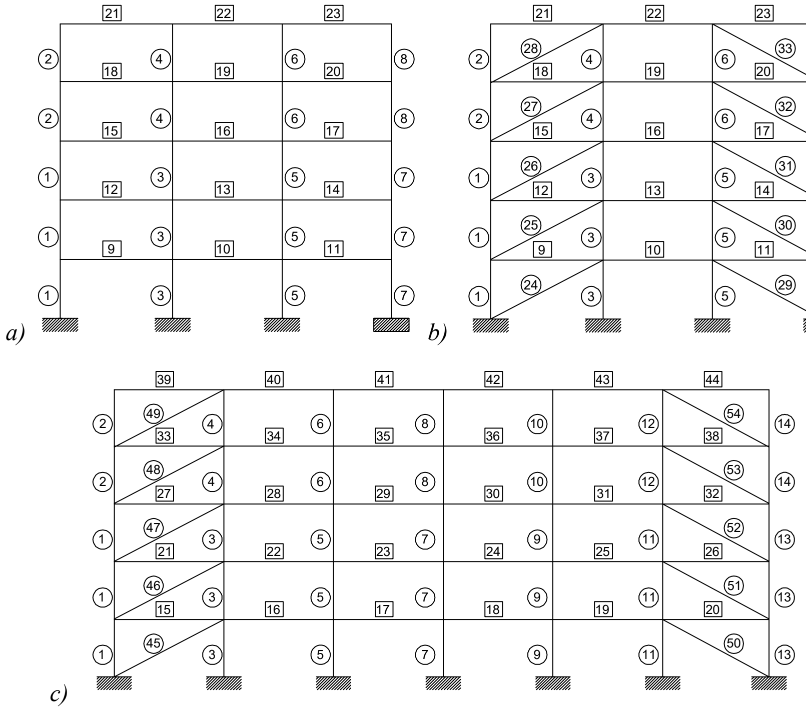

Figure 14: Frame 1 and Frame 2: a) MRF in frame 1; b) CB in frame 2; c) CB in frame 1 and 2; identification of structural members.

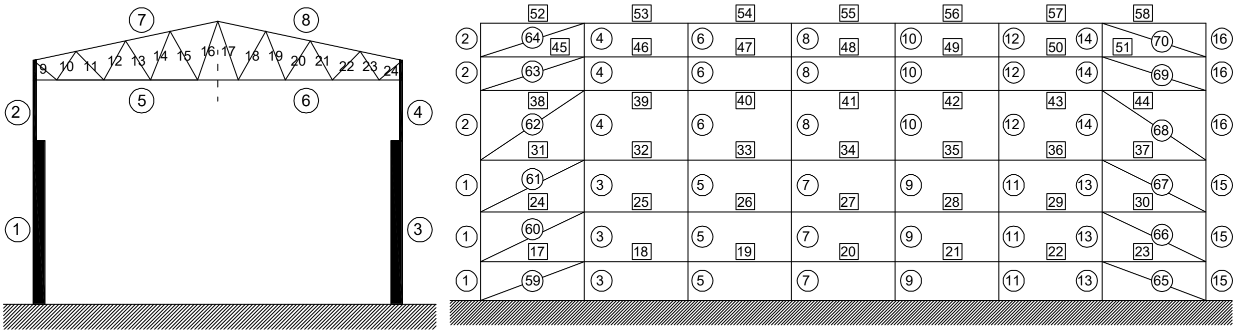

Figure 15: Frame 14: a) main trussed frame, b) CB frame.

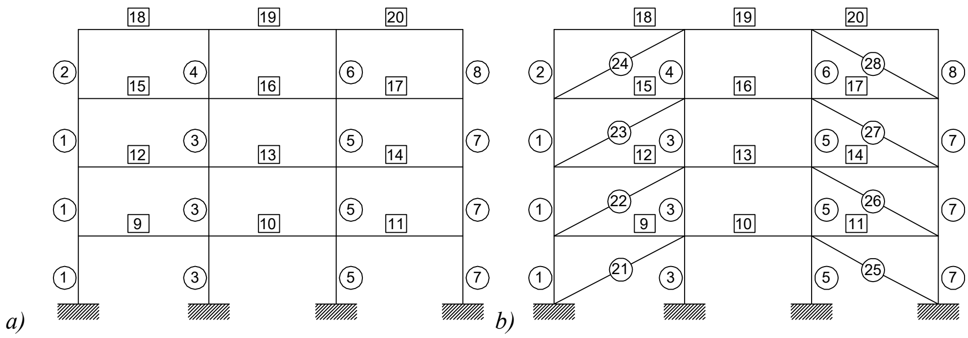

Figure 16: Frame 15 – industrial storage building: a) MRF in low seismicity areas; b) CB in low seismicity areas.

Table 22: Influence of upper yielding limits on the failure probability.

γ_{ov}	14 MRFX S355		15 MRFX S355	
Element	1-bot	3-bot	3a-top	5a-top
-	1,91E-04	2,03E-04	8,73E-07	8,62E-07
1,375	2,03E-04	2,03E-04	8,73E-07	8,60E-07
1,300	2,04E-04	2,05E-04	8,94E-07	9,13E-07
1,250	2,05E-04	2,05E-04		

8. Conclusions and implications for EN1998-1

The study reported in this paper analysed in details the influence of materials properties variation on the seismic performance of steel and steel-concrete structures. Analysed structural solutions were obtained combining different lateral resisting systems (MRF, EBF and CBF), different steel qualities (S235, S275, S355 and S460) and adopting bare steel and steel-concrete composite solutions. A total of 15 tri-dimensional regular case-study structures were designed and their mechanical response and collapse modes characterised in detail. A probabilistic procedure was set-up in order to estimate the failure probability associated to the identified collapse modes. Moreover, in order to properly include the materials properties variability in the probabilistic procedure, a model of the mechanical properties – f_y, f_t, ε_u – of the European structural steel products (profiles, plates and reinforcing bars) was calibrated.

It's necessary to underline that conclusions below presented are referred to data coming from analyzed structures, that, as previously presented, are characterized by regular shape and distribution of masses, while probably some additional consideration shall be made concerning buildings with irregular plan and/or elevation.

The first round of analyses carried out using the probabilistic procedure showed that the structural design method proposed by the Eurocodes, and in particular by the EN1998:2005, guarantees a safety level consistent with the seismic safety levels usually accepted in the literature (Melchers, 2002) for the considered buildings.

The probabilistic procedure was then applied for a second set of analyses in which a "fictitious production control" on the steel products was introduced. It was simulated the limitation of the upper yielding of the structural steels produced in accordance to the EN10025:2004, introducing different maximum limits: $f_{y,max}<1.375f_{y,nom}$; $f_{y,max}<1.350f_{y,nom}$; $f_{y,max}<1.30f_{y,nom}$; $f_{y,max}<1.25f_{y,nom}$. The production was conditioned through the rejection of all the steel samples used for realising the "dissipative elements" in the structural cases and exceeding the maximum limits.

The limitation of the maximum yielding in dissipative zones produced two opposite effects: a decrease of failure probability in protected members and a contemporary increase of failure probability associated to the ductile failure modes. This effect was evident in those cases in which the design lead to the absence of any over-sizing, while in the other cases, the effect was less evident due to over-sizing often due to extremely demanding service limit states. The use of high-strength steel qualities compared to the usual structural steel qualities gave a clear decrement of the estimated failure probability.

Aforementioned results suggested possible improvements in the seismic design procedure of the EN1998. The material over-strength factor γ_{OV} shall be differentiated according to the adopted steel quality. Moreover, the default value shall be quantitatively assessed for each quality in order to find a balance between the associated failure probabilities of ductile and not-ductile failure modes.

9. References

- Abaqus, Users' manual. Hibbitt, Karlsson, and Sorensen, Inc.; 2005.
- AFNOR, NF A 35-019-1 – 11/2007: Aciers pour béton armé – Aciers soudables à empreintes Partie 1: Barres et couronnes, 2007, France
- Badalassi M., Braconi A., Caprili S., Salvatore W. (2011). *Influence of steel mechanical properties on EBF seismic behaviour.* COMPDYN 2011, 3rd ECCOMAS Thematic Conference on Computational Methods in Structural Dynamics and Earthquake Engineering, Corfù, Greece, May 2011.
- Badalassi M., Braconi A., Caprili S., Salvatore W. (2013). Influence of steel mechanical properties on EBF seismic behaviour. *Bulletin of Earthquake Engineering*, 11:2249–2285.
- Braconi A, Bursi O.S., Fabbrocino G, Salvatore W, Taucer F, Tremblay R. Seismic performance of a 3D full-scale high-ductility steel-concrete composite moment-resisting structure - Part II: Test results and analytical validation. Earthquake Engineering & Structural Dynamics, 2008, 37:1635–1655.
- Braconi A, Bursi OS, Fabbrocino G, Salvatore W, Tremblay R. Seismic performance of a 3D full-scale high-ductility steel-concrete composite moment-resisting structure - Part I: Design and testing procedure. Earthquake Engineering & Structural Dynamics, 2008, 37:1609–1634.
- Braconi A., Caprili S., Degee H., Guendel M., Hjaij M., Hoffmeister B., Karamanos S.A., Rinaldi V., Salvatore W. (2015). Efficiency of Eurocode 8 design rules for steel and steel-concrete composite structures. *Journal of Constructional Steel Research* 112, 108–129.
- Braconi A., Caprili S., Degee H., Guendel M., Hjaij M., Hoffmeister B., Karamanos S.A., Rinaldi V., Salvatore W. (2013). *Design and assessment of steel and steel-concrete composite structures: efficacy of EN1998 design procedure,* COMPDYN 2013, 4th ECCOMAS Thematic Conference on Computational Methods in Structural Dynamics and Earthquake Engineering, Kos Island, Greece, June 12-14, 2013.
- Braconi A., Finetto M., Degee H., Hausoul N., Hoffmeister B., Gundel M., Karamanos S.A., Pappa P., Varelis G., Rinaldi V., Obiala R., Hjaij M., Somja H., Badalassi M., Caprili S., Salvatore W. (2013b). Optimizing the seismic Performance of steel and steel-composite concrete structures by Standardizing material quality control, (OPUS) Final Report. European Commission, Directorate-General for Research and Innovation, Directorate G — Industrial Technologies, Unit G.5 — Research Fund for Coal and Steel, EUR 25893 EN.
- Breitung K. (1984). Asymtotic approcimations for multinormal integrals, Journal of Engineering Mechanics, ASCE, 115(7):1577-1582.

- Cajot L.G., Haller M., Conan Y., Sedlacek G., Kraus O., Rondla J., Cerfontaine F., Lagerqvist O., Johansson B. (2005). Probabilistic quantification of safety of a steel structure highlighting the potential of steel versus other materials, PROQUAM Final Report, European Commission – Directorate-General for Research, EUR 21695 E.
- D.M. 14/01/2008 – Norme tecniche per le costruzioni, 2008, Italia.
- Denoel V. (2007). An introduction to Reliability Analysis, University of Liege, ArGEnCo.
- Ellingwood B., Galambos T.V., MacGregor J.G., Cornell C.A. (1980). *Development of a Probability Based Criterion for American National Standard A58 - Building Code Requirements for Minimum Design Loads in Buildings and Other Structures.* National Bureau of Standards, Washington.
- Elnashai A.S., Chryssanthopoulos M. (1991). Effect of random material variability on seismic design parameters of steel frames, *Earthquake engineering and structural dynamics*, 20, 101-114.
- EN10025-1÷6 General technical delivery conditions for: non-alloy, normalized/normalized rolled weldable fine grain, thermomechanical rolled weldable fine grain, improved atmospheric corrosion resistance, flat products of high yield strength in the quenched and tempered condition. European Committee for Standardization, Brussels.
- EN10219:2006. Cold formed welded structural hollow sections of non-alloy and fine grain steels. European Committee for Standardization, Brussels, 2006.
- EN1990:2005. Eurocode Basis of structural design. Technical Commission 250, Brussels, 2005.
- EN1991-1-1:2005. Eurocode 1 – Actions on structures. Part 1-1: General actions - Densities, self-weight, imposed loads for buildings, Technical Commission 250, Brussels, 2005.
- EN1992-1-1:2005. Eurocode 2 – Design of reinforced and prestressed concrete structures. Part 1-1: General rules and rules for buildings. CEN, Brussels, 2005.
- EN1993-1-1:2005. Eurocode 3 – Design of steel structures. Part 1-1: General rules and rules for buildings. Technical Commission 250/SC3, Brussels, 2005.
- EN1994-1-1:2005. Eurocode 4 – Design of composite steel and concrete structures. Part 1-1: General rules and rules for buildings. Technical Commission 250/SC4, Brussels, 2005.
- EN1998-1:2005. Eurocode 8 - Design of structures for earthquake resistance. Part 1: General rules, seismic actions and rules for buildings. Technical Commission 250/SC8, Brussels, 2005.
- EN1998-3:2005. Eurocode 8: Design of structures for earthquake resistance - Part 3: Assessment and retrofitting of buildings, Technical Commission 250/SC8, Brussels, 2005.
- FEMA 356:2000. ASCE - Prestandard and commentary for the seismic rehabilitation of buildings.
- FineLg User's Manual, V9.2. Greisch Info – Department ArGEnCo – ULg, 2003.
- Hasofer A.M., Lind N. (1974). An Exact and Invariant First-Order Reliability Format. *Journal of Engineering Mechanics,* ASCE, 100, EM1:111-121.
- JCCS (2001). Probabilistic model code 12th Draft, Parts 1–3, Joint Committee of Structural Safety, Zurich, Switzerland.
- Kuck J, Hoffmeister B. (1993). User manual for DYNACS - A Program for DYnamic Nonlinear Analysis of Composite and Steel structures (unpublished).
- Mazzoni S, McKenna F, Scott MH et al. (2007). Opensees command Language Manual.
- Melchers R. E. (2002). Structural Reliability Analysis and Prediction – 2nd Edition, John Wiley &Sons, Chichester, England.
- Menegotto M, Pinto P. (1973). Method of analysis for cyclically loaded reinforced concrete plane frame including changes of geometry and non elastic behaviour of elements under combined normal force and bending, IABSE Symposium on resistance and ultimate deformability of structures acted on by well defined repeated loads, Lisbon.
- Pinto P.E., Giannini R., Franchin P. (2004). Seismic reliability analysis of structures. IUSS Press, Pavia.
- Porter K., Scawthorn C., Taylor C. Blais N. (1998). Appropriate Seismic Reliability for Critical Equipment Systems – Recommendations Based on Regional Analysis of Financial and Life Loss, NCEER Project Numbers 94-6201 and 95-6201, MCEER, State University of New York at Buffalo.
- Porter K.A. (2003). An overview of PEER's Performance-based earthquake engineering methodology, ICASP9, Civil Engineering Risk and Reliability Association (CERRA), San Francisco, CA, July 6-9
- Rossi P.P., Lombardo A. (2007). Influence of the link overstrength factor on the seismic behaviour of eccentrically braced frames. *Journal of Constructional Steel Research*, 63:1529–1545.
- Schäfer D., Eichler B., Amlung L., Vayas I., Karlos V., Spiliopoulos A., Lippe M., Kubon Z., Kander L. (2010). Modern plastic design for steel structure, PLASTOTOUGH Final Report, European Commission – Directorate-General for Research and Innovation, EUR 24227 E.
- Somja H., Nofal S., Hjiaj M., Degee H. (2013). Effect of the steel material variability on the seismic capacity design of steel-concrete composite structures: a parametric study. Bulletin of Earthquake Engineering, 11, 1099-1127.
- Spaethe G. (1992). Die Sicherheit tragender Baukonstruktionen, Springer-Verlag Wien New York, 1992.

- UNE 36065: 2000 EX, Barras corrugadas de acero soldable con características especiales deductilidad para armaduras de hormigón armado, AEN/CTN 36 – SIDERURGIA, Espana
- Vanmarcke E.H., Gordon G.A., Heredia-Zavoni E. (1999). SIMQKE-II, conditioned earthquake ground motion simulator: user's manual, version 2.1. Princeton University, US.

Appendix

Steel Quality	Prod.	t [mm]		Mean	St. dev.	5% Perc.	95% Perc.	Curtosi	Skewness	CoV	n°	Production standard
		Min	Max	[MPa]	[MPa]	[MPa]	[MPa]					
S235J0JR (+M)(*)	A	3	16	238,8	15,9	306,0	357,5	-0,138	0,337	0,048	312	EN10025-2
S355J0 (+M)	A	3	16	414,1	21,6	379,7	449,0	-0,144	0,108	0,052	314	EN10025-2
S460M	A	3	16	495,3	17,2	469,6	525,0	0,043	0,517	0,035	113	EN10025-4
S235J0JR (+M)	A	16	40	327,7	22,8	294,7	369,0	0,067	0,350	0,039	294	EN10025-2
S275J0JR (+M)	A	16	40	349,3	33,1	303,0	414,0	0,572	0,803	0,095	915	EN10025-2
S355J2K2 (+M)	A	16	40	454,9	27,6	407,0	497,0	-0,324	-0,191	0,061	8207	EN10025-2
S460M	A	16	40	521,1	26,8	474,0	566,0	0,027	-0,023	0,051	778	EN10025-4
S275M	B	3	16	361,8	22,9	326,4	403,0	-0,140	0,030	0,063	2125	EN10025-4
S355M	B	3	16	396,5	11,8	375,4	413,0	-0,670	-0,230	0,030	61	EN10025-4
S355J0JR	C	16	40	395,6	16,2	-	-	-	-	0,041	9127	EN10025-2

Table A 1:Yielding stress ($R_{e,H}-f_y$) for structural steel profiles; (*) this class can be adopted also for S275J0JR quality

Steel Quality	Prod.	t [mm]		Mean	St. dev.	5% Perc.	95% Perc.	Curtosi	Skewness	CoV	n°	Production standard
		Min	Max	[MPa]	[MPa]	[MPa]	[MPa]					
S235J0JR (+M)(*)	A	3	16	435,4	11,2	417,6	453,5	0,993	0,586	0,026	312	EN10025-2
S355J0 (+M)	A	3	16	546,2	18,4	517,0	577,4	0,491	-0,243	0,034	314	EN10025-2
S460M	A	3	16	621,0	16,2	596,0	648,0	-0,306	-0,152	0,026	113	EN10025-4
S235J0JR (+M)	A	16	40	436,3	13,7	413,0	459,4	1,010	-0,270	0,031	294	EN10025-2
S275J0JR (+M)	A	16	40	471,9	18,3	444,0	504,0	1,536	0,581	0,039	915	EN10025-2
S355J2K2 (+M)	A	16	40	546,8	24,5	507,0	585,0	-0,579	-0,065	0,045	8207	EN10025-2
S460M	A	16	40	615,0	30,3	562,9	664,3	-0,076	-0,002	0,050	778	EN10025-4
S275M	B	3	16	479,4	12,8	460,3	503,3	0,070	0,460	0,063	2125	EN10025-4
S355M	B	3	16	574,3	11,9	551,7	590,6	1,030	-0,780	0,021	61	EN10025-4
S355J0JR	C	16	40	525,3	15,1	-	-	-	-	0,029	9127	EN10025-2

Table A 2: Tensile strength (R_m-f_t) for structural steel profiles; (*) this class can be adopted also for S275J0JR quality.

Steel Quality	Prod.	t [mm]		Mean	St. dev.	5% Perc.	95% Perc.	Curtosi	Skewness	CoV	n°	Production standard
		Min	Max	[MPa]	[MPa]	[MPa]	[MPa]					
S235J0JR (+M)(*)	A	3	16	35,0	1,6	31,9	37,4	0,573	-0,487	0,045	312	EN10025-2
S355J0 (+M)	A	3	16	27,3	1,6	24,3	29,6	1,068	-0,632	0,058	314	EN10025-2
S460M	A	3	16	24,8	1,3	22,5	26,6	1,607	-0,929	0,051	113	EN10025-4
S235J0JR (+M)	A	16	40	32,2	1,6	29,5	34,3	0,826	-0,592	0,050	294	EN10025-2
S275J0JR (+M)	A	16	40	29,7	2,1	26,2	33,1	0,120	-0,155	0,070	915	EN10025-2
S355J2K2 (+M)	A	16	40	25,9	1,8	23,3	29,4	0,293	0,632	0,070	8207	EN10025-2
S460M	A	16	40	23,4	1,6	20,7	25,9	0,510	0,049	0,070	778	EN10025-4
S275M	B	3	16	33,9	1,7	30,6	36,3	0,920	-0,620	0,051	2125	EN10025-4
S355M	B	3	16	27,8	1,8	24,9	30,7	-0,040	0,500	0,066	61	EN10025-4
S355J0JR	C	16	40	28,3	2,1	-	-	-	-	0,073	9127	EN10025-2

Table A 3: Table 23: Elongation at fracture ($A-\varepsilon_u$) for structural steel profiles; (*) this class can be adopted also for S275J0JR.

Steel Quality	t [mm]		Mean	St. dev.	5% Perc.	95% Perc.	Curtosi	Skewness	CoV	n°	Production standard
	Min	Max	[MPa]	[MPa]	[MPa]	[MPa]					
S235	7	16	351,7	28,0	308,3	407,9	0,679	0,613	0,080	84	EN10025-2
S235	16	40	345,0	28,8	296,0	389,0	-0,108	-0,301	0,083	412	EN10025-2

S235	40	63	333,3	33,1	285,0	369,0	1,927	-1,347	0,099	21	EN10025-2
S275	7	16	397,6	45,0	329,0	474,0	-0,222	0,223	0,113	278	EN10025-2
S275	16	40	387,6	36,4	327,6	451,0	0,183	0,365	0,094	437	EN10025-2
S275	40	63	372,3	28,9	326,0	431,1	0,124	0,530	0,077	120	EN10025-2
S275	63	80	373,0	27,5	344,8	430,1	1,918	1,431	0,074	55	EN10025-2
S275	80	100	363,3	23,2	341,2	418,0	2,656	1,517	0,064	45	EN10025-2
S355	7	16	487,1	41,9	416,0	553,1	-0,565	-0,021	0,086	320	EN10025-2
S355	16	40	460,6	32,4	404,0	515,0	-0,037	0,139	0,070	877	EN10025-2
S355	40	63	429,8	28,1	388,7	473,9	0,387	0,480	0,065	135	EN10025-2
S355	63	80	426,6	34,2	377,0	487,0	-0,656	0,287	0,080	91	EN10025-2
S355	80	100	456,0	32,6	421,8	492,0	-1,789	0,059	0,071	5	EN10025-2
S355W	7	16	500,4	38,1	441,8	554,1	-1,126	0,023	0,076	47	EN10025-5
S355W	16	40	469,4	30,7	421,0	522,6	-0,221	0,098	0,065	130	EN10025-5
S355W	40	63	434,8	30,1	399,2	481,0	-1,472	0,260	0,069	25	EN10025-5
S460M	16	40	492,5	18,4	470,5	515,8	0,280	0,282	0,037	6	EN10025-4
S460M	40	63	486,4	26,3	430,0	525,5	0,068	-0,366	0,054	91	EN10025-4

Table A 4: Yielding stress ($R_{e,H}-f_y$) for structural steel plates.

Steel Grade	t [mm]		Mean	St. dev.	5% Perc.	95% Perc.	Curtosi	Skewness	CoV	n°	Production standard
	Min	Max	[MPa]	[MPa]	[MPa]	[MPa]					
S235	7	16	430,6	20,5	402,0	465,0	-0,988	0,109	0,080	84	EN10025-2
S235	16	40	345,0	28,8	401,0	468,0	-0,918	-0,238	0,083	412	EN10025-2
S235	40	63	440,4	20,2	399,0	462,0	0,582	-0,965	0,099	21	EN10025-2
S275	7	16	488,0	35,1	426,0	542,2	-0,784	-0,158	0,113	278	EN10025-2
S275	16	40	387,6	36,4	432,0	530,2	-0,028	0,043	0,094	437	EN10025-2
S275	40	63	475,0	23,4	440,0	517,1	-0,013	0,330	0,077	120	EN10025-2
S275	63	80	477,9	20,2	456,7	516,9	3,076	1,505	0,074	55	EN10025-2
S275	80	100	475,3	19,5	442,6	516,6	1,643	0,257	0,064	45	EN10025-2
S355	7	16	565,7	31,9	507,0	618,0	-0,535	-0,258	0,086	320	EN10025-2
S355	16	40	460,6	32,4	507,8	598,0	-0,424	-0,102	0,070	877	EN10025-2
S355	40	63	538,4	23,9	502,0	578,3	-0,045	0,370	0,065	135	EN10025-2
S355	63	80	532,7	31,2	492,5	587,0	1,379	-0,219	0,080	91	EN10025-2
S355	80	100	542,8	32,2	511,4	583,2	-0,331	0,686	0,071	5	EN10025-2
S355W	7	16	592,8	24,2	549,0	627,4	0,578	-0,686	0,076	47	EN10025-5
S355W	16	40	568,9	30,1	518,5	619,6	-0,408	-0,065	0,065	130	EN10025-5
S355W	40	63	539,7	24,3	502,8	573,6	-1,233	-0,008	0,069	25	EN10025-5
S460M	16	40	584,2	18,9	565,0	610,3	-0,204	0,777	0,037	6	EN10025-4
S460M	40	63	580,4	23,7	537,0	621,5	0,594	0,277	0,054	91	EN10025-4

Table A 5: Tensile strength (R_m-f_t) for structural steel plates.

Steel Grade	t [mm]		Mean	St. dev.	5% Perc.	95% Perc.	Curtosi	Skewness	CoV	n°	Production standard
	Min	Max	[MPa]	[MPa]	[MPa]	[MPa]					
S235	7	16	29,0	1,02	28,0	-	-1,093	-0,966	0,080	84	EN10025-2
S235	16	40	354,0	28,80	27,0	30,0	2,958	-0,003	0,083	412	EN10025-2
S275	7	16	25,6	1,54	24,0	28,0	0,385	0,543	0,113	278	EN10025-2
S275	16	40	387,6	36,38	24,0	28,0	12,241	2,167	0,094	437	EN10025-2
S275	40	63	24,8	1,02	23,0	26,0	-0,780	0,292	0,077	120	EN10025-2
S275	63	80	24,4	1,25	22,0	26,0	-0,223	-0,030	0,074	55	EN10025-2
S275	80	100	23,8	1,03	22,0	25,0	-1,127	-0,207	0,064	45	EN10025-2
S355	7	16	24,8	1,16	23,0	26,0	0,297	0,151	0,086	320	EN10025-2
S355	16	40	460.62	32,44	23,0	27,0	1,747	0,516	0,070	877	EN10025-2
S355	40	63	24,9	1,32	22,0	27,0	0,446	-0,214	0,065	135	EN10025-2
S355	63	80	24,7	2,70	22,0	30,0	1,879	1,379	0,080	91	EN10025-2
S355	80	100	325,0	2,55	-	-	-	-	0,071	5	EN10025-2
S355W	7	16	24,5	1,36	23,0	27,3	0,956	1,004	0,076	47	EN10025-5
S355W	16	40	24,6	0,94	23,0	26,0	-0,308	0,256	0,065	130	EN10025-5
S355W	40	63	23,7	0,90	22,5	25,0	-0,054	-0,344	0,069	25	EN10025-5
S460M	16	40	24,8	4,05	20,3	30,0	-1,106	0,298	0,370	6	EN10025-4
S460M	40	63	21,9	2,64	18,2	27,5	0,996	0,839	0,054	91	EN10025-4

Table A 6: Elongation at fracture (A– ε_u) for structural steel plates.

Compressive Strength				
Concrete class		C20/25	C25/30	C30/37
cubic strength - R_c	[MPa]	25	30	27
cylindrical strength - f_c	[MPa]	20	25	30
Mean value - f_{cm}	[MPa]	36,5	40,03	41,57
Standard deviation - σ_{fcm}	[MPa]	5,7	6,21	5,22
CoV	[-]	0,159	0,155	0,126
5% percentile	[MPa]	25,36	29,93	33,05
95% percentile	[MPa]	44	29,93	49,67
Numerousness	[-]	184	334	244

Table A 7: Statistical data characterizing the concrete classes consider in the case studies design.

B450C		f_y (R_e) - Yielding Stress							f_u (R_m) - Tensile Stress							ε_{uk} (A_{gt}) - Elongation at maximum load						
ϕ	n°	Mean	St. dev.	5% Perc.	95% Perc.	Skewness	Curtosi	CoV	Mean	St. dev.	5% Perc.	95% Perc.	Skewness	Curtosi	CoV	Mean	St. dev.	10% Perc.	90% Perc.	Skewness	Curtosi	CoV
[mm]		[MPa]	[MPa]	[MPa]	[MPa]	[-]	[-]	[-]	[MPa]	[MPa]	[MPa]	[MPa]	[-]	[-]	[-]	[%]	[%]	[%]	[%]	[-]	[-]	[-]
12	237	527,2	16,9	494,8	551,2	-0,626	0,034	0,032	635,1	21,0	600,8	667,2	-0,192	-0,361	0,033	13,1	1,3	10,8	15,0	-0,208	-0,222	0,096
14	1416	523,5	15,0	497,0	547,0	-0,261	0,029	0,029	626,9	17,3	601,0	656,0	0,301	-0,086	0,028	13,3	1,1	11,9	14,6	-0,344	0,654	0,083
16	2829	521,7	12,3	499,0	540,0	-0,389	0,031	0,024	627,0	15,5	602,0	653,0	0,304	0,741	0,025	13,5	1,1	11,6	15,1	-0,189	0,931	0,080
18	519	524,6	13,1	500,8	546,0	-0,227	0,504	0,025	631,1	17,4	605,9	665,0	0,505	-0,350	0,028	13,0	1,2	11,0	14,6	-0,410	-0,314	0,091
20	1407	527,5	13,5	503,0	547,0	-0,243	0,021	0,026	631,0	13,4	609,0	653,0	0,132	0,150	0,021	13,0	1,1	11,2	14,6	0,060	0,137	0,082
24	639	537,9	15,0	512,9	560,0	-0,427	0,102	0,028	637,2	14,9	612,0	660,1	0,066	-0,059	0,023	13,1	1,0	11,3	14,6	-0,048	0,280	0,076
26	1062	535,6	14,1	511,0	557,0	-0,413	0,399	0,026	635,8	14,8	613,0	660,0	-0,099	-0,335	0,023	13,4	1,1	11,6	15,0	-0,233	0,027	0,079
30	129	529,5	15,6	501,0	553,6	-0,386	-0,258	0,029	634,0	14,0	612,0	656,0	-0,039	-0,179	0,022	13,6	1,0	12,0	15,2	-0,380	1,056	0,073
B500SD		f_y (R_e) - Yielding Stress							f_u (R_m) - Tensile Stress							ε_{uk} (A_{gt}) - Elongation at maximum load						
8	1000	561,5	22,7	525,0	597,0	-0,100	-0,130	0,040	675,5	21,5	641,0	712,0	0,150	0,090	0,032	22,9	2,9	20,0	27,5	0,560	0,250	0,126
10	1404	555,0	19,7	522,2	589,0	0,240	0,030	0,035	670,5	20,3	636,0	706,0	0,180	0,110	0,030	22,7	2,1	20,0	26,0	0,560	2,640	0,093
12	2891	559,3	18,2	529,0	589,0	-0,040	0,020	0,033	669,5	18,3	640,0	701,0	0,150	0,040	0,027	22,3	1,8	20,0	25,0	0,510	1,320	0,092
16	2896	561,3	18,7	531,0	592,0	-0,080	-0,020	0,033	670,4	20,1	640,0	705,0	0,320	0,090	0,030	21,0	2,1	17,5	23,8	0,450	1,040	0,097
20	1392	562,3	15,1	532,0	585,0	-0,410	0,880	0,027	666,4	16,2	639,0	693,0	-0,350	0,890	0,024	19,9	1,9	17,0	23,0	0,660	1,040	0,095
25	696	555,7	15,8	531,8	582,0	-0,030	-0,180	0,028	661,1	16,2	635,0	688,0	-0,080	-0,100	0,024	19,2	2,0	16,8	24,0	1,190	2,820	0,104
32	524	556,5	19,1	526,2	586,0	-0,060	-0,030	0,034	664,1	18,3	636,0	693,9	0,060	0,440	0,028	19,4	1,4	17,5	21,9	0,870	1,060	0,072
B500B		f_y (R_e) - Yielding Stress							f_u (R_m) - Tensile Stress							ε_{uk} (A_{gt}) - Elongation at maximum load						
14	1413	572,2	19,6	538,4	602,7	-0,257	0,134	0,034	672,5	19,6	637,7	701,5	-0,255	1,158	0,029	16,2	1,8	13,8	18,6	-0,014	-0,377	0,111
16	2002	579,3	17,8	549,6	607,3	0,009	0,456	0,041	674,9	17,9	646,4	704,7	0,040	0,375	0,027	15,0	1,8	12,6	17,4	0,101	-0,348	0,122
18	88	581,9	27,7	530,7	619,8	-0,350	-0,548	0,048	677,2	27,0	634,7	714,6	-0,413	-0,437	0,038	15,0	2,3	11,6	18,1	0,067	-0,525	0,155
20	2601	580,5	19,1	546,7	611,1	-0,257	0,374	0,033	678,8	20,4	647,2	714,1	0,228	0,127	0,030	16,5	1,7	14,2	18,7	-0,257	-0,047	0,104
22	48	589,7	20,5	557,4	619,7	-0,104	-0,956	0,035	689,5	18,5	653,9	711,2	-0,675	-0,314	0,027	15,5	1,8	13,4	17,7	-0,123	-0,492	0,115
25	2152	578,9	20,8	545,4	616,3	0,191	0,181	0,036	678,8	21,4	646,3	716,7	0,295	0,373	0,031	16,4	2,0	13,7	19,0	0,120	-0,211	0,124

Table A 8: Statistical parameters of rebars mechanical properties (B450C, B500B, B500S)

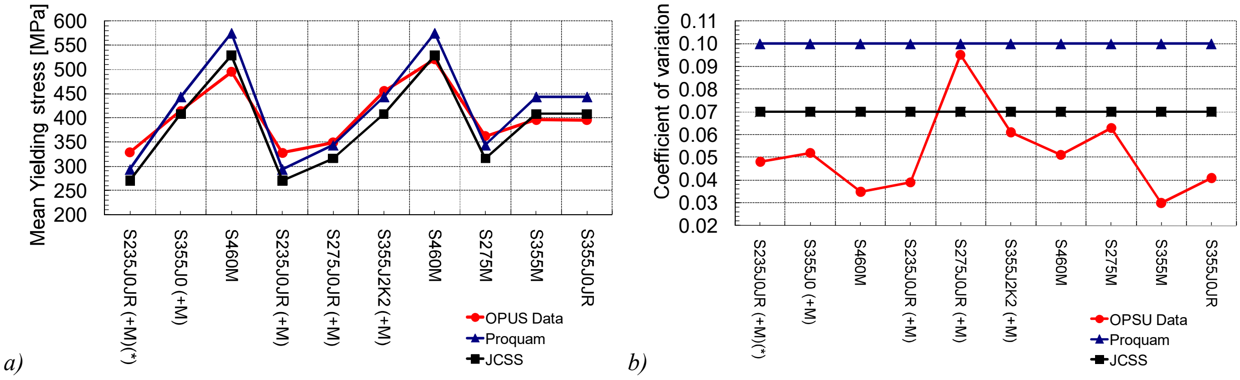

Figure A 1: Comparison between models and statistical data: a) mean and b) CoV. of yielding stress for structural steels.

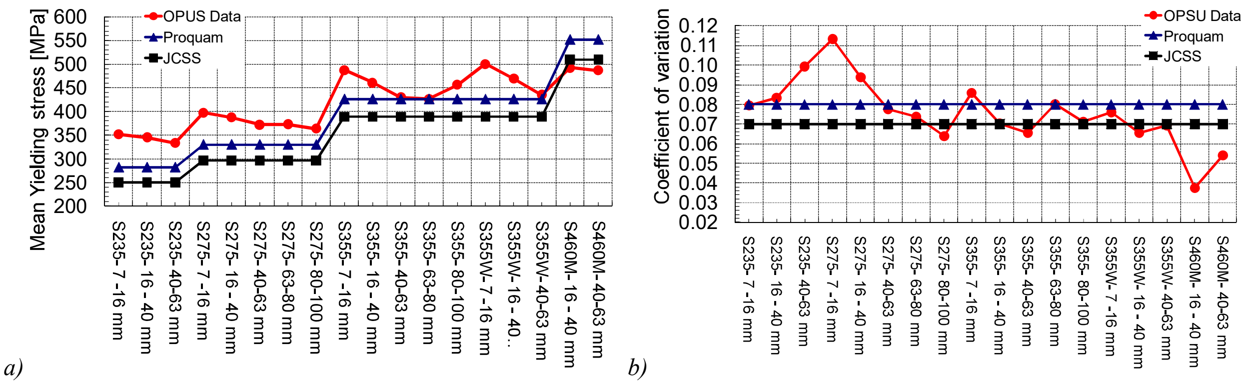

Figure A 2: Comparison between models and statistical data: a) mean and b) CoV. of yielding stress for steel plates.

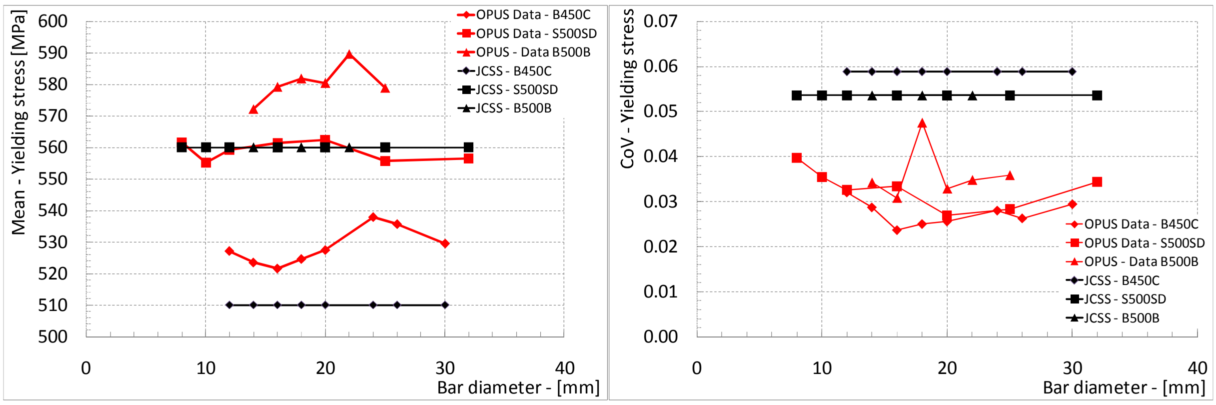

Figure A3: Comparison between models and statistical data: a) mean and b) CoV. of yielding stress.